We appreciate Referee #2 for the thoughtful and detailed comments. We revised the manuscript accordingly. We present our responses and changes below. Reviewers' comments and suggestions are in *italic*. Authors' responses are in **bold**.

Response to Referee #2:

The manuscript Reconciling the differences between OMI-based and EPA AQS in situ NO2 trends by Zhang et al. is an investigation of the differences between trends in tropospheric NO2 columns derived from the OMI satellite instrument and those derived from the EPA AQS network. This is an important and interesting research question, as in remote areas one often has to rely on remote sensing data in order to get reliable measurements of air quality. The manuscript falls well within the scope of AMT.

That being said, the manuscript fails to convince the reader regarding the comparability of the two datasets to begin with. Also, the manuscript is often too imprecise.

Most of the following points are minor and can be fixed by providing more precise information about what the authors did exactly, but they should be addressed before publication in AMT:

1 Comparing VCDs and surface concentrations

The authors fail to convince the reader why OMI VCDs, which are the integrated NO2 content of the troposphere at a given location, should be comparable to the in-situ surface concentrations of the AQS dataset. There have been numerous studies trying to relate the two measures to each other, and it should be clear to the authors that in order to compare the two, one has to take special caution. This becomes most problematic in the discussion of the effect of the lightning filter, where the authors leave the impression that lightning leads to "wrong" OMI VCDs.

As our research focuses on the regional relative trend difference, we expect that the surface NO_2 trends and NO_2 VCD trends should be very close (They are both affected by chemical non-linearity and may show trends different from emission trends). We stated this in Section 3.1, "The NO_2 relative trends from both datasets are expected to be close on a regional basis where surface emissions of NOx dominate the observed surface concentrations and tropospheric VCDs of NO_2.**" We showed in this paper what improvements can be made further, the physical reasons, and the implications for understanding regional NO_2 trends.**

To deal with the surface measurement representativeness, we only compare to regional trends from surface observations, which are much more statistically representative. Previous studies did the same. As discussed above, we show the effects of site locations on the trend analysis in Fig. 10 (and Table 1). This point has not been emphasized previously and needs to be accounted for in future studies.

We added in the abstract "However, the current OMI tropospheric NO_2 retrievals are not designed for analyzing multi-year tropospheric NO_2 trends." **It is not surprising that satellite data need to be reprocessed in trend analysis, which is true for all observation-based trend studies. We made strong points that standard OMI tropospheric NO_2 VCD data will introduce errors. We believe that our analysis results support these points.**

Having said that, we understand the reviewer's point on lightning NOx. We clarified the discussion by adding "While lightning NOx is part of OMI NO_2 observations, we treat the influence of lightning on the OMI tropospheric VCD trend as a bias for comparison purposes in this study since AQS data are not as strongly affected by lightning."

We added in the conclusions "While lightning NOx is part of OMI NO_2 observations, we treat the influence of lightning on the OMI tropospheric VCD trend as a bias for comparison purposes in this study since AQS data are not as strongly affected by lightning. Furthermore, lightning NOx effects need to be removed when

using satellite observations to understand the effects of changing anthropogenic emissions."

In a revised manuscript, the authors should include a summary of the problems arising from comparing the integrated satellite to the in-situ point measurements, should reference relevant literature, and should make sure that they consider these differences in the comparisons of the relative trends. Also, they should explicitly discuss the problems arising from comparing relative trends of these two different measures.

Table 1 shows that even though the annual trends for coincident data can be conceived as "already good", the effects of our recommended data processing are > a factor of 2 for West, Midwest, and South (comparing the OMI column with and without the lightning filter). We now emphasize this point in the abstract and conclusions. We did not add criticisms of any specific previous study because it is inappropriate to speculate if "good" agreement between in situ and OMI trends for coincident data is the reason that previous studies did not study the data processing procedures we recommended.

We further make the points that (1) processed OMI data show smaller trends (Figure 8) and (2) using surface data alone will have a tendency to overestimate NO_2 trends (Figure 9). Lastly, Figs. 4-7 show that on a seasonal basis, the effects of the data processing we recommended can be much larger than the annual mean changes of Table (1).

The lightning leads to inaccurate OMI retrieved NO_2 VCDs. Current models have difficulty simulating lightning NOx and low-pressure system meteorology correctly across different years (as stated in Section 2.3.3 and 3.2), which affects NO_2 vertical profiles and subsequently leads to inaccurate AMFs and NO_2 VCDs.

We updated the manuscript regarding potential factors contributing to the divergence between OMI-based and in situ NO_2 trends.

"Lamsal et al. (2015) also found the divergence between the annual trends inferred from the two datasets, i.e. -4.8% yr-1 vs -3.7% yr-1 during 2005-2008, and -1.2% yr-1 vs -2.1% yr-1 during 2010-2013. There are several potential factors attributing to the discrepancies between trends from satellite and ground-based measurements: interferences by the oxidation products of NOx from the chemiluminescent instruments (Lamsal et al., 2008, 2014, 2015), the differences of sampling time between OMI (~13:30 local time) and AQS (hourly) measurements (Tong et al., 2015), a high sensitivity of NO_2 VCDs to high-altitude NO_2 in contrast to the high sensitivity of surface NO_2 concentrations to surface NOx emissions (Duncan et al., 2013; Lamsal et al., 2015), spatial representativeness of satellite pixels (Lamsal et al., 2015), and high uncertainties of satellite retrievals in clean regions (Lamsal et al., 2015).

To understand how various factors and the retrieval procedure ~~affects~~ affect the resulting OMI derived trends and their differences from those derived from the surface AQS measurements, we utilize a regional 3-D chemistry transport model (CTM), a radiative transfer model (RTM), and the Mann-Kendall method (Mann, 1945; Kendall, 1948) to calculate OMI-based NO_2 seasonal relative trends during Dec-Jan-Feb (DJF), Mar-Apr-May (MAM), Jun-Jul-Aug (JJA), and Sept-Oct-Nov (SON) (Section 2)."

2 Definition of the relative trends

• 07/05: It is not entirely clear how exactly the authors calculate the relative trends. Is it a linear trend, calculated by linear regression? By default, the Mann-Kendall test is non-parameteric. If the authors use the Sen slope estimator as relative trend, they should explicitly say so. Otherwise, the authors should explicitly say what the reference value is for the relative trends (i.e., 2005, or average of the whole period, or . . .).

Thank you. We are using Mann-Kendall method with the Sen's slope estimator. We now mention this

in the abstract and Section 3.

"The Mann-Kendall method with the Sen's slope estimator is applied to derive the NO_2 seasonal and annual trends for four regions at coincident sites during 2005-2014."

"We apply the Mann-Kendall method with the Sen's slope estimator to calculate the relative trend of NO_2 for each season, i.e. DJF, MAM, JJA, and SON, during 2005-2014. We ~~construct~~ compute the uncertainties of the trends with 95th percentile confidence intervals using the Mann-Kendall method ~~a confidence level of 95%~~."

• *In some places, the authors do give an uncertainty of relative trends. However, they do not give enough detail about how these trend uncertainties are being calculated. If they indeed use the Sen slope estimator from the Mann-Kendall test as relative trend, it is unclear how they define the uncertainty of this estimate. This is however crucial in order to evalue if the improvements in the agreement of OMI and AQS relative trends are statistically significant at all. Furthermore, in some Figure captions the authors indicate 95% confidence intervals; please briefly describe in the text how these are derived.*

We use Mann-Kendall method with the Sen's slope estimator to estimate the relative trends. The uncertainties are given as the 95th percentile confidence intervals. We now state this in Section 3: "We compute the uncertainties of the trends with the 95th percentile confidence intervals using the Mann-Kendall method."

• *Another point regarding the trend calculations is the uncertainties of the relative trends. The notion of difference between OMI and AQS trends only makes sense if there is some way of assessing if these differences are statistically significant at all.*

The uncertainties, the 95th percentile confidence intervals, are shown as the error bars in Figure 7.

3 Importance of yearly varying NOx emissions

05/04: The authors claim that the yearly variations of [. . .] anthropogenic emission changes have little impact on trend analysis results, and they cite a paper by Lamsal et al. (2015). However, in the cited paper, Lamsal et al. state (Sect. 2.2.1):

In this work, we further improve the operational OMI NO2 retrieval [. . .] by using new a priori NO2 profiles [. . .] with year-specific emissions. The year-specific emissions not only improve the representation of the NO2 vertical distribution, but also capture the yearly changes in NO2 profile shapes. The latter is critical due to rapid decline in the U.S. NOx emissions in recent years [. . .].

Since the present study deals with the time period 2005–2014, I do not see how the authors' choice to use fixed 2010 NOx emissions is backed by the cited work by Lamsal et al. Given the fact that the study period does include the years of economic crisis, the authors' choice to use fixed emissions is questionable. I strongly suggest some quantitative assessment of the influence of using fixed emissions.

Lamsal et al. (2015) reported that using 2005 emission profile results in an underestimation of generally less than 2% of the overall 2005-2010 NO_2 reduction in polluted regions and that the trend is less sensitive to the vertical profile assumption in highly polluted areas (Section 2.2.2 and Figure 3, Lamsal et al., 2015). This equals to an underestimation of about 0.3% yr^{-1}, which could be used to explain the residual discrepancy (0.0-0.4% yr^{-1}) between OMI-based and in situ NO_2 trends.

The proper way to estimate the effects of NOx emissions on NO_2 VCDs is to perform NOx emission daily retrieval inversion modeling (Gu et al., 2014) to derive daily NOx emissions. We added this point to the last sentence in the conclusions. However, obtaining more reliable satellite NO_2 retrievals (as in this study) is a prerequisite to such NOx emission inversion (for trend analysis).

We revised the sentence in Section 2.3, as follows:

"The yearly variations of meteorology and anthropogenic emission changes have little impact in polluted areas on trend analysis results using OMI data (Lamsal et al., 2015)."

We revised one sentence in Section 3.1.3, as follows:

"The remaining seasonal difference of the trends reflects in part the nonlinear photochemistry (Gu et al., 2013) and the effects of NOx emission changes on NO_2 retrievals (Lamsal et al., 2015)."

4 Reconciling chemiluminescent and photolytic in-situ measurements

The authors claim that calculating a correction factor for the chemiluminescent in-situ data by taking the average ratio of chemiluminescent to photolytic measurements. This would only work properly if the reasons for the high bias of the former instruments were identical at all measurement stations. While it is true that this correction does not influence the relative trends, the authors should at least mention this.

Thank you. We now clarify this in Section 2.1, as follows:

"We correct the chemiluminescent NO_2 data by the observed ratio assuming that the inter-annual change is small and the high bias of the chemiluminescent measurements is identical at all sites."

5 Importance of individual sources of AMF uncertainty

04/28: The authors claim that the first two factors are most important for the NO_2 trend analysis, but fail to back up their claim.

We revised this sentence as follows:

"We find that the ~~The~~ NO_2 VCD trend analysis is particularly sensitive to the first two factors and we will discuss these in the following sections."

6 Time span of lightning filter

06/20: The authors' choice of lightning filter (72hrs / 90km) seems arbitrary and needs to be justified. As the authors correctly state, the lifetime of NOx in the free troposphere can reach up to one week. By making their filter only 90km wide, a back-of-the envelope calculation quickly shows that the NOx produced by a single lightning occurrence can easily be transported considerably further within 72hrs than only 90km. The authors seem to be aware of this inconsistency, because they introduce an additional filter for the Northeast which depends on lightning occurrence in the South, implying a transport distance of many hundreds of kilometers.

We have stated this in Section 2.3.3, "Since lightning usually occur along the track of a thunderstorm, the 90 km radius is more a constraint on lightning NOx effects across the track. The extended period of 72 hours

is to ensure that we exclude data affected by lightning NOx.**". We chose such filter constraints in order to balance between data availability and validity. The current constrains of 72 hours and a 90 km radius can ensure enough data (remove 2-27% data). Increasing the radius greatly will remove too much data. We discussed that our lightning filter is crude and needs improvements.**

7 Minor comments

• *04/18: NO2 partial VCDs*

Revised as suggested.

• *05/06: Which trends? Those with the default albedo, or those with the update? . . .)*

Revised as follows:

"The derived tropospheric NO2 VCD relative trends with default surface reflectance are referred as "Standard"."

• *05/09: I personally find the name ocean trend misleading, as it has nothing to do with the ocean (except for the geographical location of the clean background region). Maybe the authors can come up with a name that somehow indicates the origin of the trend (e.g., instrument drift).*

The relative trend in remote ocean potentially may stem from the similar reasons as the "hot" pixels of OMI. However, the nature of this trend is not fully understood. Thus, we decide to use the term 'ocean trend' to indicate that this trend is calculated at clean ocean region.

• *07/10: It seems that there are four different OMI-based NO2 trends*

We revised this sentence as follows:

"The ocean trend removal, MODIS albedo update, and lightning filter are then added in sequence to compute three different OMI-based NO_2 trends (in addition to "Standard") to compare to the AQS in situ results."

• *07/15: To avoid confusion, please explicitly mention that these are absolute differences of the relative trends.*

We now clarify this as follows:

"OMI-based trends generally underestimate the decreasing trends by up to 3.7% yr^{-1} (the absolute difference between relative trends) except for the large overestimation in the Midwest and the Northeast regions during DJF."

• *09/05: trends of OMI data are less — than what?*

We revised this sentence to prevent ambiguity.

"Without the lightning filter, AQS decreasing trends are stronger ~~while~~ than the decreasing trends of OMI data ~~are less~~ (Fig. 7)."

• 09/07: OMI VCDs are not overestimated when not filtering for lightning NOx - the lightning NOx is part of the VCD. It leads to worse agreement between OMI and AQS trends, but then again, these are two fundamentally different measures anyways.

Yes, but for trend analysis, lightning signals need to be removed because they are sporadic and mask out the trends due to anthropogenic emission changes in an unpredictable manner.

• 09/11: What is a reduction of decreasing surface trends? Misleading phrase, since the trends are decreasing trends to begin with. Maybe it'd be better to say stronger decreasing trends or something similar.

We revised the term accordingly.

"Therefore, the ~~reduction of~~ weaker decreasing surface trends likely reflects a reduction of low-pressure dilution effect."

• 09/12: Again, OMI VCDs are not biased due to lightning, see above.

We see the reviewer's point here. We clarified the discussion by adding "While lightning NOx is part of OMI NO_2 observations, we treat the influence of lightning on the OMI tropospheric VCD trend as a bias for comparison purposes in this study since AQS data are not as strongly affected by lightning."

We added in the conclusions "While lightning NOx is part of OMI NO_2 observations, we treat the influence of lightning on the OMI tropospheric VCD trend as a bias for comparison purposes in this study since AQS data are not as strongly affected by lightning. Furthermore, lightning NOx effects need to be removed when using satellite observations to understand the effects of changing anthropogenic emissions."

• 09/13: reduction of decreasing trends — see above

We revised the term accordingly.

"Similarly, as anthropogenic emissions decrease, the positive bias of tropospheric VCDs due to lightning NOx becomes larger, likely resulting in ~~reduction of~~ weaker decreasing trends."

• 09/15: OMI VCDs are not wrong when they include lightning NOx – the authors should therefore not make the qualitative statement corrected here. Filtered would be better.

Revised as suggested.

"We consider the lightning effects on surface NO2 trends to be mostly meteorological driven not by lightning NOx directly (e.g., Ott et al., 2010; Lu et al., 2017) and hence the ~~corrected~~ filtered OMI NO_2 data are likely

closer to emission related concentration changes."

• 09/29: I would assume that the driving factor in stronger decreasing trends close to anthropogenic source regions is the decreasing emissions in those, resulting in less transported NOx in those areas.

If the atmospheric lifetime of NOx is the spatially homogeneous and the predominant source is anthropogenic, the reduction of NOx emissions will result in the same reduction (relative change) of NOx concentrations in rural and urban regions alike. The chemical non-linearity leads to changing atmospheric lifetime of NOx in response to NOx emission changes and subsequent more evident reduction in urban areas. Also, in rural areas where the dominant NOx sources are biogenic, such as, soil and lightning, the NOx concentration relative changes will be smaller if the reduction (relative change) of NOx emissions are the same. We have already stated these in Section 3.2: "The larger decrease near the anthropogenic source regions reflect in part the nonlinear photochemistry (Gu et al., 2013) and in part to a stronger influence of NOx sources such as soils in rural regions."

• 10/03: Since comparing VCDs to surface concentrations is a difficult issue to begin with, I would not blame the OMI retrievals for the differences – when comparing apples and oranges, why should one blame one and not the other for the differences? Saying that the OMI data are not designed for trend analysis doesn't make sense. If one has to design a dataset in order to be able to do trend analysis, maybe there just are no significant trends in the underlying data to begin with?

We have to disagree. All observation data need to be corrected when they are used for trend analysis. OMI retrievals are no different. It is more complex than, say, global surface temperature data because the retrieval is much more complex. Even for something as simple as surface temperature, one must be very careful when using the observation-based trends (especially for the early part of the dataset).

• In Fig. 1a-d, it is not clear if positive numbers mean that the OMI trend or the AQS trend is higher. Please update the Figure caption with a mathematically precise description (e.g., "OMI relative trend minus AQS relative trend").

We updated the caption as follows:

"Panel (a) through (d) show the regional difference (OMI-based relative trends minus AQS relative trends) of annual relative trends between coincident OMI-based and AQS in situ data."

• Fig. 3: Please update the Figure caption with a precise indication of the units, e.g., "number of days [. . .] per REAM grid cell". Also, please spell out cloud-to-ground instead of CG in the caption.

Revised as suggested.

"Number of days with NLDN detected cloud-to-ground (CG) ~~CG~~ lightning per model grid cell per year during 2005-2014. The lightning occurrences are calculated using the REAM grid resolution."

• Fig. 6: Please indicate NO2 somewhere in the Figure caption. Also, the legend for the OMI data should be something like OMI (lightning filter); after all, the data show trends of OMI NO2 columns and not of the lightning filter.

We revised the legend and the caption.

"Seasonal relative trends of NO2 calculated from the AQS in situ measurements ("AQS", black line) and those derived from OMI data after applying the lightning filter ("OMI (lightning filter)", red line). The error bars represent 95th percentile confidence intervals. The coincident data points are less than those used in Figure 5 and therefore the AQS trends are not the same. ~~Same as Figure 5 but for coincident AQS (black line) and OMI data (redline) after applying the lightning filter. The coincident data points are less than used in Figure 5 and therefore the AQS trends are not the same.~~"

• Fig. 7: I don't understand what the figure legends are the same as in Figs. 6 and 8 is supposed to mean. Please clarify.

• Fig. 7: Please explicitly indicate in the Figure caption if statistically insignificant trends are shown or not.

We corrected the typos regarding the Figs. 4 and 6. We further clarified the confidence intervals of the error bars as follows:

"The error bars represent 95th percentile confidence intervals. The relative trends are shown in Figs. ~~6~~4 and ~~8~~6. The figure legends are the same as in Figs. ~~6~~4 and ~~8~~6 but with the AQS trends subtracted from the OMI-based trends."

• Fig. 9a: There is something wrong with the Figure caption, it does not contain a complete sentence (maybe there's just a of missing?). Please indicate what the barbs on the individual data points mean.

Revised as follows:

"(a) The "Lightning filter" OMI-based NO_2 relative trend as a function 2005-2014 averaged OMI tropospheric NO2 VCD… The error bars represent 95th percentile confidence intervals. ~~Red~~The red line shows a least-squares regression."

• Fig. 9b: Please be specific about which OMI NO2 data you show in this Figure, using the nomenclature from earlier. As explained above, the notion of corrected is misleading.

Revised as follows:

"The corrected OMI tropospheric NO_2 data ("Lightning filter") are used."

Reconciling the differences between OMI-based and EPA AQS in situ NO_2 trends

Ruixiong Zhang[1], Yuhang Wang[1], Charles Smeltzer[1], Hang Qu[1], William Koshak[2], K. Folkert Boersma[3,4]

[1]School of Earth and Atmospheric Sciences, Georgia Institute of Technology, Atlanta, Georgia, USA
[2]NASA-Marshall Space Flight Center, National Space Science & Technology Center, 320 Sparkman Drive, Huntsville, Alabama, USA
[3]Meteorology and Air Quality Group, Wageningen University, the Netherlands
[4]Royal Netherlands Meteorological Institute, De Bilt, the Netherlands

Correspondence to: Yuhang Wang (yuhang.wang@eas.gatech.edu)

Abstract. With the improved spatial resolution than earlier instruments and more than ten years of service, tropospheric NO_2 retrievals from the Ozone Monitoring Instrument (OMI) have led to many influential studies on the relationships between socioeconomic activities and NOx emissions. However, the current OMI tropospheric NO_2 retrievals are not designed for analyzing multi-year tropospheric NO_2 trends. This study focuses on how to improve OMI NO_2 retrievals for more reliable trend analysis. We retrieve OMI tropospheric NO_2 vertical column densities (VCDs) and obtain the NO_2 seasonal trends over the United States, which are compared with coincident in situ surface NO_2 measurements from the Air Quality System (AQS) network. The Mann-Kendall method with the Sen's slope estimator is applied to derive the NO_2 seasonal and annual trends for four regions at coincident sites during 2005-2014. The OMI-based NO_2 seasonal relative trends are generally biased high compared to the in situ trends by up to 3.7% yr^{-1}, except for the underestimation in the Midwest and Northeast during Dec-Jan-Feb (DJF). We improve the OMI retrievals for trend analysis by removing the ocean trend, using the MODerate-resolution Imaging Spectroradiometer (MODIS) albedo data in air mass factor (AMF) calculation, and applying a lightning flash filter to exclude lightning affected OMI NO_2 retrievals. These improvements result in close agreement (within 0.3% yr^{-1}) between in situ and OMI-based NO_2 regional annual relative trends. ~~Thus, we~~The derived OMI-based annual regional NO_2 trends change by a factor of > 2 for the South, the Midwest, and the West and seasonal changes can be even larger. We recommend future studies to apply these procedures to ensure the quality of satellite-based NO_2 trend analysis, especially in regions without reliable long-term in situ NO_2 measurements. We derive optimized OMI-based NO_2 regional annual relative trends using all available data for the West (-2.0%±0.3 yr^{-1}), the Midwest (-1.8%±0.4 yr^{-1}), the Northeast (-3.1%±0.5 yr^{-1}), and the South (-0.9%±0.3 yr^{-1}). The OMI-based annual mean trend over the contiguous United States is -1.5%±0.2 yr^{-1}. It is a factor of 2 lower than that of the AQS in situ data (-3.9%±0.4 yr^{-1}); the difference is mainly due to the fact that the locations of AQS sites are concentrated in urban and suburban regions.

1 Introduction

Nitrogen dioxide (NO_2) is an air pollutant. At high concentrations, it aggravates respiratory diseases and can lead to acid rain formation (e.g., Lamsal et al., 2015). It is also a key player to produce another pollutant, ozone (O_3), through photochemical reactions in the presence of Volatile Organic Compounds (VOCs) under sunlight. Tropospheric NO_2 is emitted both anthropogenically and naturally (e.g., Gu et al., 2016). Anthropogenic fossil fuel combustions and biomass burnings emit mostly nitrogen monoxide (NO) under high temperature, which is later oxidized by O_3 into NO_2. Major natural NO_2 sources include lightning and soils.

Surface NO_2 concentrations are regulated by the U.S. Environmental Protection Agency (EPA) through the National Ambient Air Quality Standards (NAAQS). NO_2 is measured routinely at the EPA Air Quality System (AQS) sites (Demerjian, 2000). Although the AQS network continually provides valuable hourly NO_2 measurements, AQS sites are mostly located in urban and suburban regions, leaving large regions of rural areas unmonitored. Satellite data provide a better spatial coverage than the in situ measurements.

Several satellites were launched to monitor tropospheric NO_2 vertical column densities (VCDs), such as the SCanning Imaging Absorption spectroMeter for Atmospheric CHartographY (SCIAMACHY), the Global Ozone Monitoring Experiment–2 (GOME-2), and the Ozone Monitoring Instrument (OMI). For trend analysis, the tropospheric NO_2 products from OMI surpass the others for a relatively high spatial resolution and over one decade of continuous operation (Boersma et al., 2004; Boersma et al., 2011). Thus, OMI NO_2 retrievals are widely applied in NO_2 and NOx emission trend studies (e.g., Lin et al., 2010, 2011; Castellanos et al., 2012; Russell et al., 2012; Gu et al., 2013; Lamsal et al., 2015; Lu et al., 2015; Tong et al., 2015; Cui et al., 2016; Duncan et al., 2016; de Foy et al., 2016a, 2016b; Krotkov et al., 2016; Liu et al., 2017). Tong et al. (2015) reported that the reduction rates calculated from OMI NO_2 VCDs and AQS surface NO_2 data at eight cities were -35% and -38% from 2005 to 2012, respectively. Lamsal et al. (2015) also found the divergence between the annual trends inferred from the two datasets, i.e. -4.8% yr^{-1} vs -3.7% yr^{-1} during 2005-2008, and -1.2% yr^{-1} vs -2.1% yr^{-1} during 2010-2013. There are several potential factors attributing to the discrepancies between trends from satellite and ground-based measurements: interferences by the oxidation products of NOx from the chemiluminescent instruments (Lamsal et al., 2008, 2014, 2015), the differences of sampling time between OMI (~13:30 local time) and AQS (hourly) measurements (Tong et al., 2015), a high sensitivity of NO_2 VCDs to high-altitude NO_2 in contrast to the high sensitivity of surface NO_2 concentrations to surface NOx emissions (Duncan et al., 2013; Lamsal et al., 2015), spatial representativeness of satellite pixels (Lamsal et al., 2015), and high uncertainties of satellite retrievals in clean regions (Lamsal et al., 2015).

To understand how various factors and the retrieval procedure ~~affects~~affect the resulting OMI derived trends and their differences from those derived from the surface AQS measurements, we utilize a regional 3-D chemistry transport model (CTM), a radiative transfer model (RTM), and the Mann-Kendall method (Mann, 1945; Kendall, 1948) to calculate OMI-based NO_2 seasonal relative trends during Dec-Jan-Feb (DJF), Mar-Apr-May (MAM), Jun-Jul-Aug (JJA), and Sept-Oct-Nov (SON) (Section 2). To reconcile with the AQS

based regional NO_2 trends, we find that three procedures are essential to ensure the quality of trend analysis using OMI tropospheric NO_2 VCDs, including the ocean trend removal, the MODerate-resolution Imaging Spectroradiometer (MODIS) albedo update in calculating the air mass factors (AMFs), and the lightning filter (Section 3.1). With these procedures implemented, the differences between OMI-based and AQS in situ annual relative trends are within 0.3% yr^{-1} of coincident measurements for all the four regions. Finally, we estimate the OMI-based annual relative trends across the nation in Section 3.2. Conclusions are given in Section 4.

2 Methods

2.1 EPA AQS surface NO_2 measurements

The in situ surface NO_2 measurements from the U.S. EPA AQS network are used in this research. Sites with a continuous measurement gap of more than 50 days are removed and the observations of 140 remaining cites are used (Fig. 1). The AQS chemiluminescent analyzers are equipped with molybdenum converters to measure ambient NO_2 concentrations. These analyzers are known to have high biases, since the converters are not NO_2 specific and they measure some fractions of peroxyacetyl nitrate, nitric acid and organic nitrates (Demerjian, 2000; Lamsal et al., 2008). In addition to chemiluminescent analyzers, several NO_2 specific photolytic instruments were deployed since 2013. By utilizing the data from both chemiluminescent and photolytic measurements at coincident sites during the overpassing time of OMI, we calculate the observed NO_2 concentration ratio between both measurements in Fig. S1 in the Supplement. The ratio peaks at 2.3 in June and decreases to 1.3 in November, indicating that the chemiluminescent analyzers overestimate by 27%-132% than photolytic instruments. This finding is in agreement with Lamsal et al. (2008). We correct the chemiluminescent NO_2 data by the observed ratio assuming that the inter-annual change is small~~.~~ and the high bias of the chemiluminescent measurements is identical at all sites. This correction may contribute to the differences between in situ and OMI based absolute NO_2 trends but do not significantly affect the relative trends (since the correction is canceled out in computing relative trends). In this study, we only examine the relative trends and therefore the analysis results are not affected by the uncertainties in the in situ NO_2 measurement corrections.

2.2 REAM model

We use a 3-D Regional chEmical trAnsport Model (REAM) in the simulation of NO_2 profiles. REAM has widely been used in atmospheric NO_2 studies, including vertical transport (Choi et al., 2005; Zhao et al., 2009a; Zhang et al., 2016a), emission inversions (Zhao et al., 2009b; Yang et al., 2011; Gu et al., 2013, 2014, 2016), and regional and seasonal variations (Choi et al., 2008a, 2008b). The model has a horizontal resolution of 36 km with 30 vertical layers in the troposphere, 5 vertical layers in the stratosphere, and a model top of 10 hpa. In this study, the domain of REAM is about 400 km larger on each side than the contiguous United States (CONUS). Meteorology inputs driving transport process are simulated by the Weather Research and

Forecasting model (WRF) assimilations constrained by National Centers for Environmental Prediction Climate Forecast System Reanalysis (NCEP CFSR, Saha et al., 2010) 6-hourly products. The KF-eta scheme is used for sub-grid convective transport in WRF (Kain and Fritsch,1993). We run the WRF model with the same resolution as in REAM but with a domain 10 grids larger on each side than that of REAM. REAM updates most of the meteorology inputs every 30 minutes while those related to convective transport and lightning parameterization are updated every 5 minutes. The chemistry mechanism expands that of a global CTM GEOS-Chem (V9-02) with aromatics chemistry (Bey et al., 2001; Liu et al., 2010, 2012a, 2012b; Zhang et al., 2017). For consistency, the GEOS-Chem (V9-02) simulation with $2° \times 2.5°$ resolution is used to generate initial and boundary conditions for chemical tracers.

Anthropogenic emissions of NOx and other chemical species are from the U.S. National Emission Inventory 2008 prepared using the Sparse Matrix Operator Kernel Emission (SMOKE) model. Biogenic emissions are simulated online using the Model of Emissions of Gases and Aerosols from Nature (MEGAN) algorithm (v2.1, Guenther et al., 2012). We parameterize lightning emitted NOx as a function of convective mass flux and Convective Available Potential Energy (CAPE) (Choi et al., 2005). NOx production per flash is set to 250 moles NO per flash, and the emissions are distributed vertically following the C-shaped profiles by Pickering et al. (1998). For recent model evaluations of REAM with observations, we refer readers to Zhang et al. (2016a, 2016b), Cheng et al. (2017), and Zhang et al. (2017).

2.3 OMI-based NO_2 VCDs

We retrieve the tropospheric NO_2 VCDs using the tropospheric slant column densities (SCDs) from the Royal Dutch Meteorological Institute (KNMI) Dutch OMI NO_2 product (DOMINO v2, Boersma et al., 2011). OMI onboard the Aura satellite was launched in July 2004 and is still active. OMI overpasses the equator at about 13:30 Local Time (LT) and obtains global coverage with a 2600 km viewing swath spanning 60 rows. It has a ground level spatial resolution up to 13 km x 24 km (at nadir). The spatial extent of the OMI pixels will not affect our analysis as we focus on regional trend analysis. SCDs are retrieved by matching a modeled spectrum to an observed top-of-atmosphere reflectance with the Differential Optical Absorption Spectroscopy (DOAS) technique within a fitting window of 405-465nm. The stratospheric portion of SCDs are estimated and subsequently removed with a global CTM TM4 with stratospheric ozone assimilation (Dirksen et al., 2011). Deriving tropospheric VCDs from the remaining tropospheric SCDs requires the calculation of AMFs. Being an optically thin gas, tropospheric AMF for NO_2 can be calculated from AMF for each vertical layer (AMF_l) weighted by NO_2 partial VCDs at the corresponding layer (x_l) (Boersma et al., 2004), as shown in equation (1).

$$\text{tropospheric AMF} = \frac{tropospheric\ SCD}{tropospheric\ VCD} = \frac{\int AMF_l x_l dl}{\int x_l dl} \quad (1)$$

As the vertical distribution of NO_2 is usually unknown, we typically substitute x_l by an a priori profile ($x_{l,apriori}$) from a CTM. AMF_l is the sensitivity of NO_2 SCD to VCD at a given altitude (Eskes and Boersma, 2003), and is computed using the Double Adding KNMI (DAK) RTM (Lorente et al., 2017). As a result, the

retrieved tropospheric NO_2 VCD computation depends on the a priori NO_2 vertical profile, the surface reflectance, the surface pressure, the temperature profile, and the viewing geometry (Boersma et al., 2011). Previous studies have addressed the sources of uncertainties in NO_2 retrievals, including surface reflectance resolutions (Russell et al., 2011; Lin et al., 2014), lightning NOx (Choi et al., 2005a; Martin et al., 2007; Bucsela et al., 2010), a priori CTM uncertainties (Russell et al., 2011; Heckel et al., 2011; Lin et al., 2012; Laughner et al., 2016), surface pressure and reflectance anisotropy in rugged terrain (Zhou et al., 2009), cloud and aerosol radiance (Lin et al., 2014, 2015), and boundary layer dynamics (Zhang et al., 2016a). ~~The~~We find that the NO_2 VCD trend analysis is particularly sensitive to the first two factors and we will discuss these in the following sections.

AMFs are derived using the pre-computed altitude-dependent AMF lookup table, which is generated by the DAK RTM. We use the NO_2 profiles from REAM, temperature and pressure from CSFR, viewing geometry and cloud information from DOMINO v2 product. We use the REAM results of 2010 to avoid the uncertainty introduced by yearly variation of NO_2 profiles. The yearly variations of meteorology and anthropogenic emission changes have little impact in polluted areas on trend analysis results using OMI data (Lamsal et al., 2015). We use the surface reflectance from DOMINO v2 product as default (Kleipool et al., 2008), and update it using a surface reflectance product with a higher temporal resolution (Section 2.3.2). The derived tropospheric NO_2 VCD relative trends with default surface reflectance are referred as "Standard".

2.3.1 Ocean trend removal

For trend and other analyses of OMI tropospheric VCDs, the data of anomalous pixels must be removed. The row anomaly initially occurred in June 2007 and subsequently in later years affected rows 26-40 (Schenkeveld et al., 2017). Additional anomalies can be found in some years in rows 41-55. For trend analysis from 2005-2014, we exclude rows 26-55, consistent with our understanding of the row anomaly (Schenkeveld et al., 2017), and following the flagging in the DOMINO v2 data product. In addition, the data of coarse spatial resolution from rows 1-5 and rows 56-60 are also excluded, as suggested by Lamsal et al. (2015). Furthermore, we exclude OMI data with cloud fraction > 0.3 to minimize retrieval uncertainties due to clouds and aerosols (Boersma et al., 2011; Lin et al., 2014).

Fig. 2a shows that there is an apparent increasing trend of the averaged tropospheric SCDs in the remote ocean region (Fig. 2b) with minimal marine traffic. This trend reflects the increase in the magnitude of the stripes (step-wise SCD variability from one row to another) in time, which originates from the use of a constant (2005-averaged) solar irradiance reference spectrum in the DOAS spectral fits throughout the mission and the weak increase of noise in the OMI radiance measurements (Boersma, personal communication, 2017; Zara et al., 2018). Fig. 2a shows that there is a positive annual trend of $1.75\pm0.45\times10^{13}$ molecules cm^{-2} yr^{-1}. The ocean trend is insensitive to the region selection in the remote North Pacific (varies within 10%). We only analyze OMI tropospheric column trends over the CONUS for grid cells with 2005-

2014 averaged VCDs > $1x10^{15}$ molecules cm^{-2}, which tends to minimize the effect of the background noise. However, removing this background ocean (absolute) trend has a non-negligible effect in reducing the OMI relative trend (Fig. 1). We refer to such derived (relative) trend data as "Ocean". An alternative method is to subtract monthly SCDs of the remote ocean region from the OMI tropospheric SCD data. Although the end results are essentially the same as the trend removal method, noises are added to the SCD data (Fig. 2a), making it more difficult to understand the effects of the MODIS albedo update and the lightning filter (next sections). We therefore choose to use the (absolute) trend removal method here.

2.3.2 MODIS albedo update

The albedo data used to calculate the AMF_l in "Standard" and "Ocean" versions of trend analysis are from the DOMINO v2 products, which are the climatology of averaged OMI measurements during 2005-2009 with a spatial resolution of 0.5°×0.5° (Kleipool et al., 2008) and is valid for 440 nm. We recalculate the AMF_l using the MODIS 16-day MCD43B3 albedo product with 1km spatial resolution, which combines data from both MODIS onboard Aqua and Terra satellites (Schaaf et al., 2002; Tang and Zhang, 2007). Aqua and Terra have an equatorial overpassing time of 13:30 LT and 10:30 LT, respectively. The band 3 (459nm-479nm) is used to match the NO_2 fitting window (405nm-465nm). The albedo is spatially integrated to the geometry of OMI pixels and is temporally interpolated to match OMI overpassing dates. In order to maintain the consistency of the DOMINO retrieval algorithm (Boersma et al., 2011), we only use the MODIS data to improve the temporal variations of albedo data used in the retrieval. We scale the MODIS albedo data such that the mean albedo during 2005-2009 is the same as the OMI climatology at 0.5°×0.5°. We recalculate OMI tropospheric VCDs using the MODIS albedo data as described. We recalculate the relative OMI trend and remove the ocean (absolute) trend (Section 2.3.1). We refer to this version of OMI relative trend data as "MODIS".

2.3.3 Lightning event filter

Over North America, lightning is a major source of NOx in the free troposphere and its simulations in CTMs are uncertain (e.g., Zhao et al., 2009a; Luo et al., 2017). The large temporospatial variations of lightning NOx make it difficult to compute satellite based NO_2 trends by changing the vertical distributions of NO_2 affecting the AMF calculation (e.g., Choi et al., 2008b; Lamsal et al., 2010) and the SCD values. Given the difficulty to simulate lightning NOx accurately across different years, we use a lightning filter to remove potential effects of lightning NOx on the basis of the flash rate observations of cloud-to-ground (CG) lightning flash data detected by the National Lightning Detection Network™ (NLDN) (Cummins and Murphy, 2009; Rudlosky and Fuelberg, 2010). NLDN only reports the ground point of a CG lightning flash, while the CG lightning flash can extend horizontally to tens of kilometers. A CG lightning flash can affect the NO_2 retrievals not only in the model grid cell where the CG lightning is located but also the nearby model grid cells. The atmospheric lifetime of NOx in the free troposphere can be up to 1 week. Therefore, we exclude the OMI NO_2 data within a radius of ~~90km~~90 km of the NLDN-reported CG lightning location (about two

model grid cells around the grid cell where the CG lightning is located) for a period of 72 hours after the lightning occurrence. Since lightning usually occur along the track of a thunderstorm, the 90 km radius is more a constraint on lightning NOx effects across the track. The extended period of 72 hours is to ensure that we exclude data affected by lightning NOx. Figure 4 shows the distribution of the number of days of 2005-2014 with lightning detection. The Southwest monsoon and the South regions have more lightning days than the other areas. While there are fewer lightning flashes in the Northeast than the South (Fig. 3), large amounts of lightning NOx can be produced by high flash ratios of severe thunderstorms and they can be transported northward from the South to the Northeast (Choi et al., 2005). We therefore further filter OMI NO_2 data in the Northeast on the basis of CG lightning flash rates in the South. If the average CG flash rate in the South exceeds the 95th percentile value of the NLDN observations, which is 0.035 flash km^{-2} day^{-1} (Fig. S2 in the Supplement), we exclude in the analysis the Northeast OMI data in the following 72 hours. Excluding the OMI data based on CG lightning data implicitly removes the data affected by cloud-to-cloud lightning collocated with CG lightning. The lightning filter removes about 2%, 27%, 20%, and 19% of OMI data, which are coincident with AQS data, for the West, the Midwest, the Northeast and the South, respectively. We refer to this version of OMI relative trend data as "Lightning filter".

3 Results and discussion

We group the analysis results into different regions: (a) West, (b) Midwest, (c) Northeast, and (d) South (Fig. 1), following the regional divisions by the United States Census Bureau. To make a fair comparison between the in situ and OMI-based trends, we only use spatially and temporally coincident in situ and OMI NO_2 observations in Section 3.1. We apply the Mann-Kendall method with the Sen's slope estimator to calculate the relative trend of NO_2 for each season, i.e. DJF, MAM, JJA, and SON, during 2005-2014. We ~~construct~~compute the uncertainties of the trends with ~~a~~the 95th percentile confidence ~~level of 95%.~~intervals using the Mann-Kendall method. Note that when we compare in situ and OMI-based trends, the lightning filter also removes in situ NO_2 data, which are coincident with the OMI NO_2 data affected by lightning. This leads to slightly different in situ NO_2 trends between Fig. 4 and Fig. 6 (Section 3.2.3). We first compute the trends using the "Standard" OMI VCD data. The ocean trend removal, MODIS albedo update, and lightning filter are then added in sequence to compute three different OMI-based NO_2 trends (in addition to "Standard") to compare to the AQS in situ results. A subtlety in the comparison is that the coincident data change when the lightning filter is applied. As a result, the AQS in situ results in this set of comparison differ from those in the other three sets.

3.1 In situ and "Standard" OMI-based trends

Fig. 4 shows that both AQS in situ and "Standard" OMI-based seasonal relative trends are negative for all seasons across the regions. OMI-based trends generally underestimate the decreasing trends by up to 3.7% yr^{-1} (the absolute difference between relative trends) except for the large overestimation in the Midwest and the Northeast regions during DJF. The overestimates in these two regions are 3.0% yr^{-1} and 1.1% yr^{-1},

respectively. On average, the differences between OMI-based and in situ seasonal relative trends are 1.6% yr^{-1}, -0.3% yr^{-1}, 1.0% yr^{-1}, and 1.4% yr^{-1} for the West, the Midwest, the Northeast, and the South regions, respectively. Note that the relative trends are calculated using coincident measurements for the comparisons. The NO_2 relative trends from both datasets are expected to be close on a regional basis where surface emissions of NOx dominate the observed surface concentrations and tropospheric VCDs of NO_2. The focus of this work is to reconcile the difference between AQS in situ and OMI-based trends, which will be discussed in the following sections.

3.1.1 Improvement due to ocean trend correction

After removing the ocean trend as discussed in Section 2.3.1, the OMI-based NO_2 decreasing trends are more pronounced as shown in Fig. 4 ("Ocean", blue line) by 0.1-0.9% yr^{-1}. The regional relative trends have different sensitivities to the ocean trend removal due to different tropospheric VCDs levels. In general, the discrepancies between OMI-based and in situ trends are reduced except for the Midwest and the Northeast regions during DJF, which are already biased low. The averaged differences between OMI-based and in situ seasonal relative trends for the West, the Midwest, the Northeast, and the South regions are 1.2% yr^{-1}, -1.1% yr^{-1}, 0.4% yr^{-1}, and 1.0% yr^{-1}. Only in the Midwest region, removing the ocean trend enlarges the difference due to the large winter bias.

3.1.2 Improvement due to MODIS albedo update

The adoption of the up-to-date MODIS albedo (Section 2.3.2) greatly reduces the difference of relative trends in the Midwest during DJF from -3.6% yr^{-1} ("Ocean") to 1.3% yr^{-1} ("MODIS"), the improvement of DJF trend difference is more moderate from -1.7% to 0.5% (Fig. 4). There are no significant changes of the comparisons in other regions or other seasons. Fig. 5 shows the albedo seasonal relative trends for the 4 regions coincident with AQS in situ NO_2 data. The OMI DOMINO v2 incorporates a climatology albedo dataset (Kleipool et al., 2008) with snow/ice albedo adjustment using the NASA Near-real-time Ice and Snow Extent (NISE) dataset (Boersma et al., 2011). The climatology albedo data exhibits no trends. Thus, the trends of albedo mainly originate from the yearly variation of NISE detected snow/ice, followed by OMI sampling variation. The noticeable seasonal trend of the OMI DOMINO v2 albedo dataset is the 3.9% yr^{-1} increase in DJF of the Midwest and a smaller DJF increase (1.0%) of the Northeast. In contrast, the MODIS albedo dataset exhibits a smaller positive DJF trend (0.8% yr^{-1}), 3.1% yr^{-1} less than the trend from DOMINO v2, in the Midwest, and a small negative DJF trend (-0.8%) in the Northeast. The comparison to the AQS data shows that the MODIS albedo update leads to better agreement between satellite and in suit trends in winter in these regions (Fig. 4).

3.1.3 Improvement due to lightning filter

As discussed in Section 2.3.3, lightning NOx affects the retrievals of satellite tropospheric NO_2 VCDs. Fig. 6 shows that the lightning filter significantly reduces the difference between the OMI-based relative trend

and that of the AQS data by 0.5-1.4% yr^{-1} in the Northeast and 0.9-1.3% yr^{-1} in the South. As a result, the seasonal trend differences are within 0.9% yr^{-1} in these two regions except during SON. The lightning filter has little effect on the West and the Midwest. While lightning NOx can be significant during the monsoon season in some regions of the West (Fig. 3), the average tropospheric NO_2 VCDs are usually < $1x10^{15}$ molecules cm^{-2} and lightning affected regions are therefore excluded in trend analysis.

The effect of lightning filter (Fig. 6) cannot be shown in Fig. 4 because the coincident OMI and AQS data points are fewer after applying the lightning filter. We examine the improvements of ocean trend removal, MODIS albedo update, and lightning filter by comparing the differences of different OMI-based seasonal relative trends from the AQS in situ trends in Fig. 7. The previously discussed improvements such as OMI albedo update for the Midwest and the Northeast during DJF are shown. By subtracting the AQS trends, we can now find clear improvements of the lightning filter for the South and the Northeast. There remains seasonal variation of OMI-based trend biases relative to in situ data but the discrepancies of the annual trends after the three discussed procedures are relatively small at 0.3% yr^{-1}, -0.3% yr^{-1}, -0.1% yr^{-1}, and 0.0% yr^{-1}, in the West, the Midwest, the Northeast, and the South regions (Fig. 1), respectively. The remaining seasonal difference of the trends reflects in part the nonlinear photochemistry (Gu et al., 2013) and the effects of NOx emission changes on NO_2 retrievals (Lamsal et al., 2015).

3.2 OMI-based NO_2 trends

Table 1 summarizes the regional annual trends of coincident AQS in situ and OMI data. The "Standard" OMI data (following the DOMINO v2 algorithm) tend to show less NO_2 reduction than AQS data. After applying the three corrections discussed in the previous section to the OMI data, the agreement with the AQS trends is within the uncertainties of the trends. While lightning NOx is part of OMI NO_2 observations, we treat the influence of lightning on the OMI tropospheric VCD trend as a bias for comparison purposes in this study since AQS data are not as strongly affected by lightning.

Without the lightning filter, AQS decreasing trends are stronger ~~while~~than the decreasing trends of OMI data ~~are less~~ (Fig. 7). The lightning trend in the NLDN data is unclear due in part to the changing instrument sensitivity (Koshak et al., 2015). If lightning NOx is not accounted for in OMI retrieval, tropospheric NO_2 VCDs are overestimated. On the other hand, lightning accompanies low pressure systems which mix the atmosphere vertically and tend to reduce surface NO_2 concentrations when anthropogenic emissions are high such as urban and suburban regions. Therefore, lightning has opposite effects on surface and satellite trends. The low-pressure dilution effect on surface NO_2 concentrations depends on anthropogenic emissions (since the end point of dilution is the background NO_2 value). Therefore, the ~~reduction of~~weaker decreasing surface trends likely reflects a reduction of low-pressure dilution effect. Similarly, as anthropogenic emissions decrease, the positive bias of tropospheric VCDs due to lightning NOx becomes larger, likely resulting in ~~a reduction of~~weaker decreasing trends. We consider the lightning effects on surface NO_2 trends to be mostly meteorological driven not by lightning NOx directly (e.g., Ott et al., 2010; Lu et al., 2017) and hence the ~~corrected~~filtered OMI NO_2 data are likely closer to emission related concentration changes.

The AQS in situ NO_2 annual relative trends (coincident with OMI data with lightning filter) are most significant in the Northeast (-5.2±0.6% yr^{-1}) and the West (-4.2±0.5% yr^{-1}), followed by the South (-3.0±0.5% yr^{-1}) and the Midwest (-2.8±0.6% yr^{-1}) regions. The nationwide annual trend is -4.1±0.4% yr^{-1}, which is consistent with the previous studies (Lamsal et al., 2015; Lu et al., 2015; Tong et al., 2015; de Foy et al., 2016b; Duncan et al., 2016; Krotkov et al., 2016). The significant NO_2 reductions result from updated technologies and strict regulations (Krotkov, et al., 2016). The corrected OMI-based NO_2 trends (coincident with AQS data) show similar reduction rates in the West (-3.8±0.4% yr^{-1}), the Midwest (-3.1±0.5% yr^{-1}), the Northeast (-5.3±0.7% yr^{-1}) and the South (-3.0±0.5% yr^{-1}) regions. The nationwide annual trend is -3.9±0.3% yr^{-1}.

One advantage of satellite observations over a surface monitoring network is spatial coverage. The OMI data ("Lightning filter") coincident with the AQS data show a national annual trend of -3.9±0.3% yr^{-1} similar to the AQS in situ trend of -4.1±0.4% yr^{-1}. Using all data available (Fig. 8, Table 1), the OMI data ("Lightning filter") show a much lower trend of -1.5±0.2%yr^{-1}, about half of the AQS trend (-3.9±0.4% yr^{-1}). Fig. 9 shows that the AQS sites, which are mostly urban and suburban sites, tend to be located in regions with high tropospheric NO_2 VCDs. The OMI decreasing trend with corrected data is a function of tropospheric NO_2 VCDs, increasing from 0% yr^{-1} to -6% yr^{-1} (Fig. 9). The national annual trend is close to the value of clean regions which contribute much more than polluted regions. The larger decrease near the anthropogenic source regions reflect in part the nonlinear photochemistry (Gu et al., 2013) and in part to a stronger influence of NOx sources such as soils in rural regions.

4. Conclusions

Using data from the DOMINO v2 algorithm, we find that the computed OMI-based seasonal NO_2 (relative) trends underestimate the decreasing trends of the EPA AQS data by up to 3.7% yr^{-1}. We attribute most of the discrepancies to OMI retrievals since the standard retrieval algorithm was not specifically designed for trend analysis. While lightning NOx is part of OMI NO_2 observations, we treat the influence of lightning on the OMI tropospheric VCD trend as a bias for comparison purposes in this study since AQS data are not as strongly affected by lightning. Furthermore, lightning NOx effects need to be removed when using satellite observations to understand the effects of changing anthropogenic emissions.

In this study, we show that removing the background ocean trend (likely a result of the increasing stripes), adopting MODIS albedo data (with better temporospatial resolutions), and excluding lightning influences can bring OMI tropospheric NO_2 VCD trends in close agreement (within 0.3% yr^{-1}) with those of the AQS data. The largest effects of MODIS albedo update are in winter in Midwest and Northeast and those of lightning filter are in the South and the Northeast. After applying these corrections, the derived OMI-based annual regional NO_2 trends change by a factor of > 2 for the South, the Midwest, and the West and seasonal changes can be even larger. We derive optimized OMI-based NO_2 regional annual relative trends using all available data for the West (-2.0%±0.3 yr^{-1}), the Midwest (-1.8%±0.4 yr^{-1}), the Northeast (-3.1%±0.5 yr^{-1}), and the South (-0.9%±0.3 yr^{-1}).

The national annual trend of the corrected OMI data is -1.5±0.2%yr^{-1}, about half of the AQS trend (-3.9±0.4% yr^{-1}). It reflects that the AQS sites are mostly located in the urban and suburban regions, where OMI data show much larger decreasing trends (up to -6% yr^{-1}) than rural regions (down to 0% yr^{-1}). The reasons for the dependence of OMI derived trends on tropospheric NO_2 VCDs and the seasonal/regional trend differences are still not completely understood. Further studies are necessary to improve our understanding of these trends. The observation-based lightning filter implemented in this study is preliminary. Incorporating chemical transport modeling may improve this filter. Moreover, the results presented here represent an alternative and indirect way to assess the importance of lightning NOx for National Climate Assessment (NCA) analyses described in Koshak et al. (2015), and Koshak (2017). Inversion studies (e.g., Zhao and Wang, 2009; Gu et al., 2013, 2014, 2016) will be needed to ~~understand~~quantify the emission and AMF changes corresponding to the OMI tropospheric NO_2 VCD trends.

Acknowledgements

This work was supported by the NASA ACMAP Program and the NASA Climate Indicators and Data Products for Future National Climate Assessments (NNH14ZDA001N-INCA). We thank data sources, including DOMINO v2 OMI data from KNMI, MODIS data from NASA, and EPA AQS NO_2 data from EPA. In addition, the authors gratefully acknowledge Vaisala Inc. for providing the NLDN data used in this study. K. Folkert Boersma acknowledges funding from the EU FP7 project QA4ECV (grant no. 607405).

Data access

The datasets used in this research have been obtained online as follows:

- DOMINO v2 NO_2 retrievals: http://www.temis.nl/airpollution/no2.html
- EPA AQS NO_2 data: US Environmental Protection Agency. Air Quality System Data Mart [internet database] available at http://www.epa.gov/ttn/airs/aqsdatamart.
- NLDN lightning data: https://lightning.nsstc.nasa.gov/data/data_nldn.html
- MODIS MCD43B3 data: https://lpdaac.usgs.gov/dataset_discovery/modis/modis_products_table/mcd43b3

References

Bey, I., Jacob, D. J., Yantosca, R. M., Logan, J. A., Field, B. D., Fiore, A. M., Li, Q. B., Liu, H. G. Y., Mickley, L. J., and Schultz, M. G.: Global modeling of tropospheric chemistry with assimilated meteorology: Model description and evaluation, J. Geophys. Res.-Atmos., 106, 23073-23095, 10.1029/2001jd000807, 2001.

Boersma, K. F., Eskes, H. J., and Brinksma, E. J.: Error analysis for tropospheric NO_2 retrieval from space, J. Geophys. Res.-Atmos., 109, 10.1029/2003JD003962, 2004.

Boersma, K. F., Eskes, H. J., Veefkind, J. P., Brinksma, E. J., van der A, R. J., Sneep, M., van den Oord, G. H. J., Levelt, P. F., Stammes, P., Gleason, J. F., and Bucsela, E. J.: Near-real time retrieval of tropospheric NO_2 from OMI, Atmos. Chem. Phys., 7, 2103-2118, 10.5194/acp-7-2103-2007, 2007.

Boersma, K. F., Eskes, H. J., Dirksen, R. J., van der A, R. J., Veefkind, J. P., Stammes, P., Huijnen, V., Kleipool, Q. L., Sneep, M., Claas, J., Leitão, J., Richter, A., Zhou, Y., and Brunner, D.: An improved tropospheric NO_2 column retrieval algorithm for the Ozone Monitoring Instrument, Atmos. Meas. Tech., 4, 1905-1928, 10.5194/amt-4-1905-2011, 2011.

Bucsela, E. J., Pickering, K. E., Huntemann, T. L., Cohen, R. C., Perring, A., Gleason, J. F., Blakeslee, R. J., Albrecht, R. I., Holzworth, R., Cipriani, J. P., Vargas-Navarro, D., Mora-Segura, I., Pacheco-Hernández, A., and Laporte-Molina, S.: Lightning-generated NOx seen by the Ozone Monitoring Instrument during NASA's Tropical Composition, Cloud and Climate Coupling Experiment (TC4), J. Geophys. Res.-Atmos., 115, 10.1029/2009JD013118, 2010.

Castellanos, P., and Boersma, K. F.: Reductions in nitrogen oxides over Europe driven by environmental policy and economic recession, Sci. Rep., 2, 265, 10.1038/srep00265, 2012.

Choi, Y., Wang, Y., Zeng, T., Martin, R. V., Kurosu, T. P., and Chance, K.: Evidence of lightning NOx and convective transport of pollutants in satellite observations over North America, Geophys. Res. Lett., 32, L02805, 10.1029/2004GL021436, 2005.

Choi, Y., Wang, Y., Zeng, T., Cunnold, D., Yang, E.-S., Martin, R., Chance, K., Thouret, V., and Edgerton, E.: Springtime transitions of NO_2, CO, and O_3 over North America: Model evaluation and analysis, J. Geophys. Res.-Atmos., 113, D20311, 10.1029/2007JD009632, 2008a.

Choi, Y., Wang, Y., Yang, Q., Cunnold, D., Zeng, T., Shim, C., Luo, M., Eldering, A., Bucsela, E., and Gleason, J.: Spring to summer northward migration of high O_3 over the western North Atlantic, Geophys. Res. Lett., 35, L04818, 10.1029/2007GL032276, 2008b.

Cui, Y., Lin, J., Song, C., Liu, M., Yan, Y., Xu, Y., and Huang, B.: Rapid growth in nitrogen dioxide pollution over Western China, 2005–2013, Atmos. Chem. Phys., 16, 6207-6221, 10.5194/acp-16-6207-2016, 2016.

Cummins, K. L., and Murphy, M. J.: An Overview of Lightning Locating Systems: History, Techniques, and Data Uses, With an In-Depth Look at the U.S. NLDN, IEEE Transactions on Electromagnetic Compatibility, 51, 499-518, 10.1109/TEMC.2009.2023450, 2009.

de Foy, B., Lu, Z., and Streets, D. G.: Satellite NO_2 retrievals suggest China has exceeded its NOx reduction goals from the twelfth Five-Year Plan, Sci. Rep., 6, 35912, 10.1038/srep35912, 2016a.

de Foy, B., Lu, Z., and Streets, D. G.: Impacts of control strategies, the Great Recession and weekday variations on NO_2 columns above North American cities, Atmos. Environ., 138, 74-86, j.atmosenv.2016.04.038, 2016b.

Demerjian, K. L.: A review of national monitoring networks in North America, Atmos. Environ., 34, 1861-1884, 10.1016/S1352-2310(99)00452-5, 2000.

Dirksen, R. J., Boersma, K. F., Eskes, H. J., Ionov, D. V., Bucsela, E. J., Levelt, P. F., and Kelder, H. M.: Evaluation of stratospheric NO2 retrieved from the Ozone Monitoring Instrument: Intercomparison, diurnal cycle, and trending, J. Geophys. Res.-Atmos., 116, 10.1029/2010JD014943, 2011.

Duncan, B. N., Yoshida, Y., de Foy, B., Lamsal, L. N., Streets, D. G., Lu, Z. F., Pickering, K. E., and Krotkov, N. A.: The observed response of Ozone Monitoring Instrument (OMI) NO2 columns to NOx emission controls on power plants in the United States: 2005-2011, Atmospheric Environment, 81, 102-111, 10.1016/j.atmosenv.2013.08.068, 2013.

Duncan, B. N., Lamsal, L. N., Thompson, A. M., Yoshida, Y., Lu, Z., Streets, D. G., Hurwitz, M. M., and Pickering, K. E.: A space-based, high-resolution view of notable changes in urban NOx pollution around the world (2005–2014), J. Geophys. Res.-Atmos., 121, 976-996, 10.1002/2015JD024121, 2016.

Eskes, H. J., and Boersma, K. F.: Averaging kernels for DOAS total-column satellite retrievals, Atmos. Chem. Phys., 3, 1285-1291, 10.5194/acp-3-1285-2003, 2003.

Gu, D. S., Wang, Y. H., Smeltzer, C., and Liu, Z.: Reduction in NOx Emission Trends over China: Regional and Seasonal Variations, Environ. Sci. Technol., 47, 12912-12919, 10.1021/es401727e, 2013.

Gu, D., Wang, Y., Smeltzer, C., and Boersma, K. F.: Anthropogenic emissions of NOx over China: Reconciling the difference of inverse modeling results using GOME-2 and OMI measurements, J. Geophys. Res.-Atmos., 119, 2014JD021644, 10.1002/2014JD021644, 2014.

Gu, D., Wang, Y., Yin, R., Zhang, Y., and Smeltzer, C.: Inverse modelling of NOx emissions over eastern China: uncertainties due to chemical non-linearity, Atmos. Meas. Tech., 9, 5193-5201, 10.5194/amt-9-5193-2016, 2016.

Guenther, A. B., Jiang, X., Heald, C. L., Sakulyanontvittaya, T., Duhl, T., Emmons, L. K., and Wang, X.: The Model of Emissions of Gases and Aerosols from Nature version 2.1 (MEGAN2.1): an extended and updated framework for modeling biogenic emissions, Geosci. Model Dev., 5, 1471-1492, 10.5194/gmd-5-1471-2012, 2012.

Heckel, A., Kim, S. W., Frost, G. J., Richter, A., Trainer, M., and Burrows, J. P.: Influence of low spatial resolution a priori data on tropospheric NO_2 satellite retrievals, Atmos. Meas. Tech., 4, 1805-1820, 10.5194/amt-4-1805-2011, 2011.

Jiakui, T., Aijun, Z., and Zhengmin, H.: The earth surface reflectance retrieval by exploiting the synergy of TERRA and AQUA MODIS data, 2007 IEEE International Geoscience and Remote Sensing Symposium, 2007, 1697-1700,

Kain, J. S., and Fritsch, J. M.: Convective Parameterization for Mesoscale Models: The Kain-Fritsch Scheme, in: The Representation of Cumulus Convection in Numerical Models, edited by: Emanuel, K. A., and Raymond, D. J., Am. Meteorol. Soc., Boston, MA, 165-170, 1993.

Kendall, M. G.: Rank correlation methods, Rank correlation methods., Griffin, Oxford, England, 1948.

Kleipool, Q. L., Dobber, M. R., de Haan, J. F., and Levelt, P. F.: Earth surface reflectance climatology from 3 years of OMI data, J. Geophys. Res.-Atmos., 113, 10.1029/2008JD010290, 2008.

Koshak, W., Peterson, H., Biazar, A., Khan, M., and Wang, L.: The NASA Lightning Nitrogen Oxides Model (LNOM): Application to air quality modeling, Atmos. Res., 135–136, 363-369, 10.1016/j.atmosres.2012.12.015, 2014.

Koshak, W. J., Cummins, K. L., Buechler, D. E., Vant-Hull, B., Blakeslee, R. J., Williams, E. R., and Peterson, H. S.: Variability of CONUS Lightning in 2003–12 and Associated Impacts, J. Appl. Meteorol. Clim., 54, 15-41, 10.1175/jamc-d-14-0072.1, 2015.

Koshak, W. J., Lightning NOx estimates from space-based lightning imagers, 16th Annual Community Modeling and Analysis System (CMAS) Conference, Chapel Hill, NC, October 23-25, 2017.

Krotkov, N., Herman, J., Bhartia, P. K., Seftor, C., Arola, A., Kaurola, J., Koskinen, L., Kalliskota, S., Taalas, P., and Geogdzhaev, I.: Version 2 TOMS UV algorithm: problems and enhancements, in: P Soc Photo-Opt Ins, edited by: Slusser, J. R., Herman, J. R., and Gao, W., Proceedings of the Society of Photo-Optical Instrumentation Engineers (Spie), Spie-Int Soc Optical Engineering, Bellingham, 82-93, 2002.

Krotkov, N. A., McLinden, C. A., Li, C., Lamsal, L. N., Celarier, E. A., Marchenko, S. V., Swartz, W. H., Bucsela, E. J., Joiner, J., Duncan, B. N., Boersma, K. F., Veefkind, J. P., Levelt, P. F., Fioletov, V. E., Dickerson, R. R., He, H., Lu, Z., and Streets, D. G.: Aura OMI observations of regional SO_2 and NO_2 pollution changes from 2005 to 2015, Atmos. Chem. Phys., 16, 4605-4629, 10.5194/acp-16-4605-2016, 2016.

Lamsal, L. N., Martin, R. V., van Donkelaar, A., Steinbacher, M., Celarier, E. A., Bucsela, E., Dunlea, E. J., and Pinto, J. P.: Ground-level nitrogen dioxide concentrations inferred from the satellite-borne Ozone Monitoring Instrument, J. Geophys. Res.-Atmos., 113, 10.1029/2007JD009235, 2008.

Lamsal, L. N., Martin, R. V., van Donkelaar, A., Celarier, E. A., Bucsela, E. J., Boersma, K. F., Dirksen, R., Luo, C., and Wang, Y.: Indirect validation of tropospheric nitrogen dioxide retrieved from the OMI satellite instrument: Insight into the seasonal variation of nitrogen oxides at northern midlatitudes, J. Geophys. Res.-Atmos., 115, 10.1029/2009JD013351, 2010.

Lamsal, L. N., Krotkov, N. A., Celarier, E. A., Swartz, W. H., Pickering, K. E., Bucsela, E. J., Gleason, J. F., Martin, R. V., Philip, S., Irie, H., Cede, A., Herman, J., Weinheimer, A., Szykman, J. J., and Knepp, T. N.: Evaluation of OMI operational standard NO2 column retrievals using in situ and surface-based NO2 observations, Atmos. Chem. Phys., 14, 11587-11609, 10.5194/acp-14-11587-2014, 2014.

Lamsal, L. N., Duncan, B. N., Yoshida, Y., Krotkov, N. A., Pickering, K. E., Streets, D. G., and Lu, Z.: U.S. NO2 trends (2005–2013): EPA Air Quality System (AQS) data versus improved observations from the Ozone Monitoring Instrument (OMI), Atmos. Environ., 110, 130-143, j.atmosenv.2015.03.055, 2015.

Laughner, J. L., Zare, A., and Cohen, R. C.: Effects of daily meteorology on the interpretation of space-based remote sensing of NO_2, Atmos. Chem. Phys., 16, 15247-15264, 10.5194/acp-16-15247-2016, 2016.

Lin, J. T., McElroy, M. B., and Boersma, K. F.: Constraint of anthropogenic NOx emissions in China from different sectors: a new methodology using multiple satellite retrievals, Atmos. Chem. Phys., 10, 63-78, 10.5194/acp-10-63-2010, 2010.

Lin, J. T., and McElroy, M. B.: Detection from space of a reduction in anthropogenic emissions of nitrogen oxides during the Chinese economic downturn, Atmos. Chem. Phys., 11, 8171-8188, 10.5194/acp-11-8171-2011, 2011.

Lin, J. T., Liu, Z., Zhang, Q., Liu, H., Mao, J., and Zhuang, G.: Modeling uncertainties for tropospheric nitrogen dioxide columns affecting satellite-based inverse modeling of nitrogen oxides emissions, Atmos. Chem. Phys., 12, 12255-12275, 10.5194/acp-12-12255-2012, 2012.

Lin, J. T., Pan, D., and Zhang, R.: Trend and Interannual Variability of Chinese Air Pollution since 2000 in Association with Socioeconomic Development: A Brief Overview, Atmos. Oceanic Sci. Lett., 6, 84-89, 10.1080/16742834.2013.11447061, 2013.

Lin, J. T., Martin, R. V., Boersma, K. F., Sneep, M., Stammes, P., Spurr, R., Wang, P., Van Roozendael, M., Clémer, K., and Irie, H.: Retrieving tropospheric nitrogen dioxide from the Ozone Monitoring Instrument: effects of aerosols, surface reflectance anisotropy, and vertical profile of nitrogen dioxide, Atmos. Chem. Phys., 14, 1441-1461, 10.5194/acp-14-1441-2014, 2014.

Lin, J. T., Liu, M. Y., Xin, J. Y., Boersma, K. F., Spurr, R., Martin, R., and Zhang, Q.: Influence of aerosols and surface reflectance on satellite NO_2 retrieval: seasonal and spatial characteristics and implications for NOx emission constraints, Atmos. Chem. Phys., 15, 11217-11241, 10.5194/acp-15-11217-2015, 2015.

Liu, F., Beirle, S., Zhang, Q., van der A, R. J., Zheng, B., Tong, D., and He, K.: NOx emission trends over Chinese cities estimated from OMI observations during 2005 to 2015, Atmos. Chem. Phys., 17, 9261-9275, 10.5194/acp-17-9261-2017, 2017.

Liu, Z., Wang, Y., Gu, D., Zhao, C., Huey, L. G., Stickel, R., Liao, J., Shao, M., Zhu, T., Zeng, L., Liu, S.-C., Chang, C.-C., Amoroso, A., and Costabile, F.: Evidence of Reactive Aromatics As a Major Source of Peroxy Acetyl Nitrate over China, Environ. Sci. Technol., 44, 7017-7022, 10.1021/es1007966, 2010.

Liu, Z., Wang, Y., Vrekoussis, M., Richter, A., Wittrock, F., Burrows, J. P., Shao, M., Chang, C.-C., Liu, S.-C., Wang, H., and Chen, C.: Exploring the missing source of glyoxal (CHOCHO) over China, Geophys. Res. Lett., 39, L10812, 10.1029/2012GL051645, 2012a.

Liu, Z., Wang, Y., Gu, D., Zhao, C., Huey, L. G., Stickel, R., Liao, J., Shao, M., Zhu, T., Zeng, L., Amoroso, A., Costabile, F., Chang, C. C., and Liu, S. C.: Summertime photochemistry during CAREBeijing-2007: ROx budgets and O3 formation, Atmos. Chem. Phys., 12, 7737-7752, 10.5194/acp-12-7737-2012, 2012b.

Lorente, A., Folkert Boersma, K., Yu, H., Dörner, S., Hilboll, A., Richter, A., Liu, M., Lamsal, L. N., Barkley, M., De Smedt, I., Van Roozendael, M., Wang, Y., Wagner, T., Beirle, S., Lin, J. T., Krotkov, N., Stammes, P., Wang, P., Eskes, H. J., and Krol, M.: Structural uncertainty in air mass factor calculation for NO2 and HCHO satellite retrievals, Atmos. Meas. Tech., 10, 759-782, 10.5194/amt-10-759-2017, 2017.

Lu, Z., Streets, D. G., de Foy, B., Lamsal, L. N., Duncan, B. N., and Xing, J.: Emissions of nitrogen oxides from US urban areas: estimation from Ozone Monitoring Instrument retrievals for 2005–2014, Atmos. Chem. Phys., 15, 10367-10383, 10.5194/acp-15-10367-2015, 2015.

Luo, C., Wang, Y., and Koshak, W. J.: Development of a self-consistent lightning NOx simulation in large-scale 3-D models, J. Geophys. Res.-Atmos., 122, 3141-3154, 10.1002/2016JD026225, 2017.

Mann, H. B.: NONPARAMETRIC TESTS AGAINST TREND, Econometrica, 13, 245-259, 10.2307/1907187, 1945.

Martin, R. V., Sauvage, B., Folkins, I., Sioris, C. E., Boone, C., Bernath, P., and Ziemke, J.: Space-based constraints on the production of nitric oxide by lightning, J. Geophys. Res.-Atmos., 112, 10.1029/2006JD007831, 2007.

Ott, L. E., Pickering, K. E., Stenchikov, G. L., Allen, D. J., DeCaria, A. J., Ridley, B., Lin, R.-F., Lang, S., and Tao, W.-K.: Production of lightning NOx and its vertical distribution calculated from three-dimensional cloud-scale chemical transport model simulations, J. Geophys. Res.-Atmos., 115, 10.1029/2009JD011880, 2010.

Pickering, K. E., Wang, Y., Tao, W.-K., Price, C., and Müller, J.-F.: Vertical distributions of lightning NOx for use in regional and global chemical transport models, J. Geophys. Res.-Atmos., 103, 31203-31216, 10.1029/98JD02651, 1998.

Rudlosky, S. D., and Fuelberg, H. E.: Pre- and Postupgrade Distributions of NLDN Reported Cloud-to-Ground Lightning Characteristics in the Contiguous United States, Mon. Weather Rev., 138, 3623-3633, 10.1175/2010mwr3283.1, 2010.

Russell, A. R., Perring, A. E., Valin, L. C., Bucsela, E. J., Browne, E. C., Wooldridge, P. J., and Cohen, R. C.: A high spatial resolution retrieval of NO_2 column densities from OMI: method and evaluation, Atmos. Chem. Phys., 11, 8543-8554, 10.5194/acp-11-8543-2011, 2011.

Russell, A. R., Valin, L. C., and Cohen, R. C.: Trends in OMI NO_2 observations over the United States: effects of emission control technology and the economic recession, Atmos. Chem. Phys., 12, 12197-12209, 10.5194/acp-12-12197-2012, 2012.

Saha, S., Moorthi, S., Pan, H.-L., Wu, X., Wang, J., Nadiga, S., Tripp, P., Kistler, R., Woollen, J., Behringer, D., Liu, H., Stokes, D., Grumbine, R., Gayno, G., Wang, J., Hou, Y.-T., Chuang, H.-Y., Juang, H.-M. H., Sela, J., Iredell, M., Treadon, R., Kleist, D., Van Delst, P., Keyser, D., Derber, J., Ek, M., Meng, J., Wei, H., Yang, R., Lord, S., Van Den Dool, H., Kumar, A., Wang, W., Long, C., Chelliah, M., Xue, Y., Huang, B., Schemm, J.-K., Ebisuzaki, W., Lin, R., Xie, P., Chen, M., Zhou, S., Higgins, W., Zou, C.-Z., Liu, Q., Chen, Y., Han, Y., Cucurull, L., Reynolds, R. W., Rutledge, G., and Goldberg, M.: The NCEP Climate Forecast System Reanalysis, Bulletin of the Am. Meteorol. Soc., 91, 1015-1057, 10.1175/2010BAMS3001.1, 2010.

Schaaf, C. B., Gao, F., Strahler, A. H., Lucht, W., Li, X., Tsang, T., Strugnell, N. C., Zhang, X., Jin, Y., Muller, J.-P., Lewis, P., Barnsley, M., Hobson, P., Disney, M., Roberts, G., Dunderdale, M., Doll, C., d'Entremont, R. P., Hu, B., Liang, S., Privette, J. L., and Roy, D.: First operational BRDF, albedo nadir

reflectance products from MODIS, Remote Sens. Environ., 83, 135-148, 10.1016/S0034-4257(02)00091-3, 2002.

Schenkeveld, V. M. E., Jaross, G., Marchenko, S., Haffner, D., Kleipool, Q. L., Rozemeijer, N. C., Veefkind, J. P., and Levelt, P. F.: In-flight performance of the Ozone Monitoring Instrument, Atmos. Meas. Tech., 10, 1957-1986, 10.5194/amt-10-1957-2017, 2017.

Tang, J. K., and Zhang, A. J.: The earth surface reflectance retrieval by exploiting the synergy of TERRA and AQUA MODIS data, Int. Geosci. Remote Se., 1697-1700, 10.1109/Igarss.2007.4423144, 2007.

Tong, D. Q., Lamsal, L., Pan, L., Ding, C., Kim, H., Lee, P., Chai, T., Pickering, K. E., and Stajner, I.: Long-term NOx trends over large cities in the United States during the great recession: Comparison of satellite retrievals, ground observations, and emission inventories, Atmos. Environ., 107, 70-84, 10.1016/j.atmosenv.2015.01.035, 2015.

Yang, Q., Wang, Y., Zhao, C., Liu, Z., Gustafson, W. I., and Shao, M.: NOx Emission Reduction and its Effects on Ozone during the 2008 Olympic Games, Environ. Sci. Technol., 45, 6404-6410, 10.1021/es200675v, 2011.

Zara, M., Boersma, K. F., De Smedt, I., Richter, A., Peters, E., Van Geffen, J. H. G. M., Beirle, S., Wagner, T., Van Roozendael, M., Marchenko, S., Lamsal, L. N., and Eskes, H. J.: Improved slant column density retrieval of nitrogen dioxide and formaldehyde for OMI and GOME-2A from QA4ECV: intercomparison, uncertainty characterization, and trends, Atmos. Meas. Tech. Discuss., 2018, 1-47, 10.5194/amt-2017-453, 2018.

Zhang, R., Wang, Y., He, Q., Chen, L., Zhang, Y., Qu, H., Smeltzer, C., Li, J., Alvarado, L. M. A., Vrekoussis, M., Richter, A., Wittrock, F., and Burrows, J. P.: Enhanced trans-Himalaya pollution transport to the Tibetan Plateau by cut-off low systems, Atmos. Chem. Phys., 17, 3083-3095, 10.5194/acp-17-3083-2017, 2017.

Zhang, Y., Wang, Y., Chen, G., Smeltzer, C., Crawford, J., Olson, J., Szykman, J., Weinheimer, A. J., Knapp, D. J., Montzka, D. D., Wisthaler, A., Mikoviny, T., Fried, A., and Diskin, G.: Large vertical gradient of reactive nitrogen oxides in the boundary layer: Modeling analysis of DISCOVER-AQ 2011 observations, J. Geophys. Res.-Atmos., 121, 1922-1934, 10.1002/2015JD024203, 2016a.

Zhang, Y., and Wang, Y.: Climate-driven ground-level ozone extreme in the fall over the Southeast United States, P. Natl. Acad. Sci., 113, 10025-10030, 10.1073/pnas.1602563113, 2016b.

Zhao, C., Wang, Y., Choi, Y., and Zeng, T.: Summertime impact of convective transport and lightning NOx production over North America: modeling dependence on meteorological simulations, Atmos. Chem. Phys., 9, 4315-4327, 10.5194/acp-9-4315-2009, 2009a.

Zhao, C., and Wang, Y.: Assimilated inversion of NOx emissions over east Asia using OMI NO_2 column measurements, Geophys. Res. Lett., 36, L06805, 10.1029/2008GL037123, 2009b.

Zhou, Y., Brunner, D., Boersma, K. F., Dirksen, R., and Wang, P.: An improved tropospheric NO_2 retrieval for OMI observations in the vicinity of mountainous terrain, Atmos. Meas. Tech., 2, 401-416, 10.5194/amt-2-401-2009, 2009.

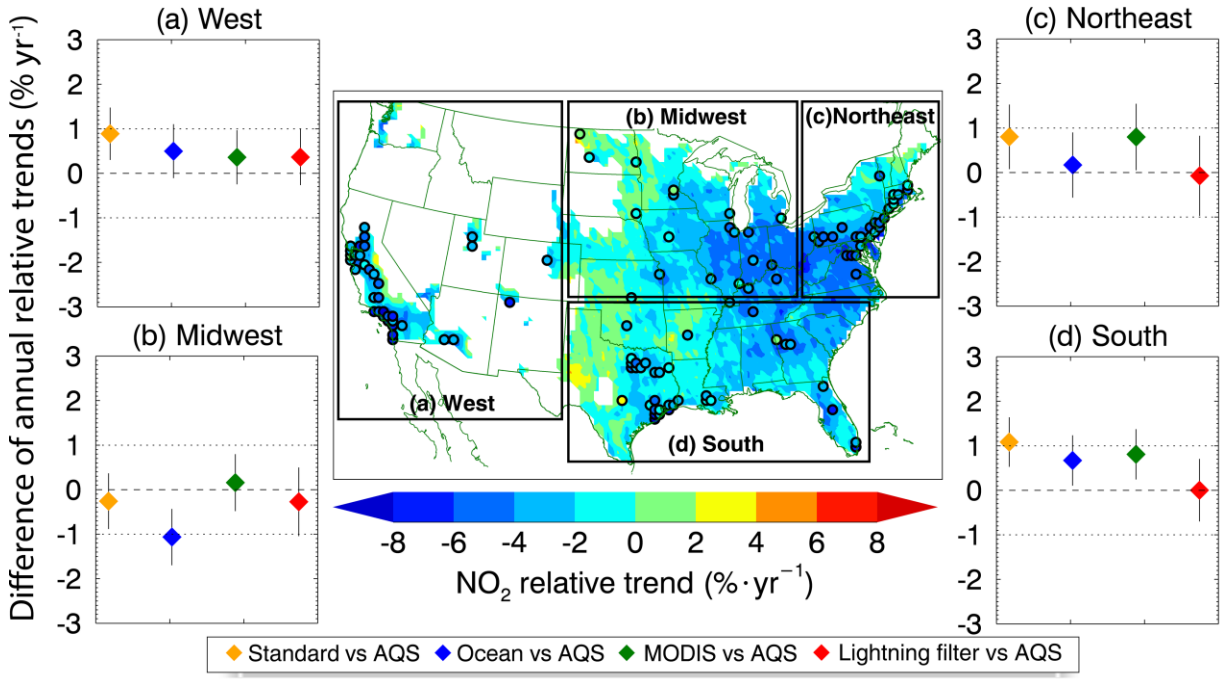

Figure 1. The solid black borders in the center map define the four regions used in this study. The colored background shows the OMI-based NO_2 annual relative trends of the "lightning filter" data. Grid cells with 2005-2014 mean NO_2 VCD values < $1x10^{15}$ molecules cm^{-2} are excluded in this study and are shown in white. The black bordered circles represent the locations of AQS sites. Panel (a) through (d) show the regional difference (OMI-based relative trends minus AQS relative trends) of annual relative trends between coincident OMI-based and AQS in situ data. The colored diamonds are for "Standard" (orange), "Ocean" (blue), "MODIS" (green), and "Lightning filter" (red) OMI data, respectively. The different OMI VCD data are described in Section 2.4.

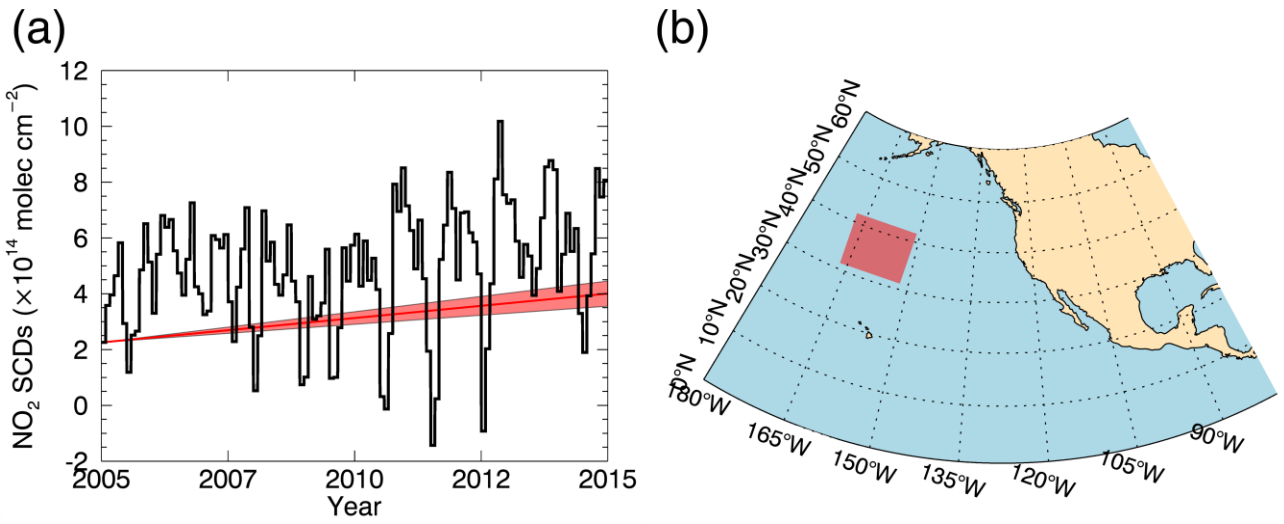

~~F~~igure 2. The black line in panel (a) shows the monthly averaged OMI tropospheric NO_2 VCD values in the North Pacific region (red box in panel (b)) from 2005 to 2014. The red line in panel (a) represents the ocean trend used in this research, with the ~~95%~~95th percentile confidence intervals shaded in red.

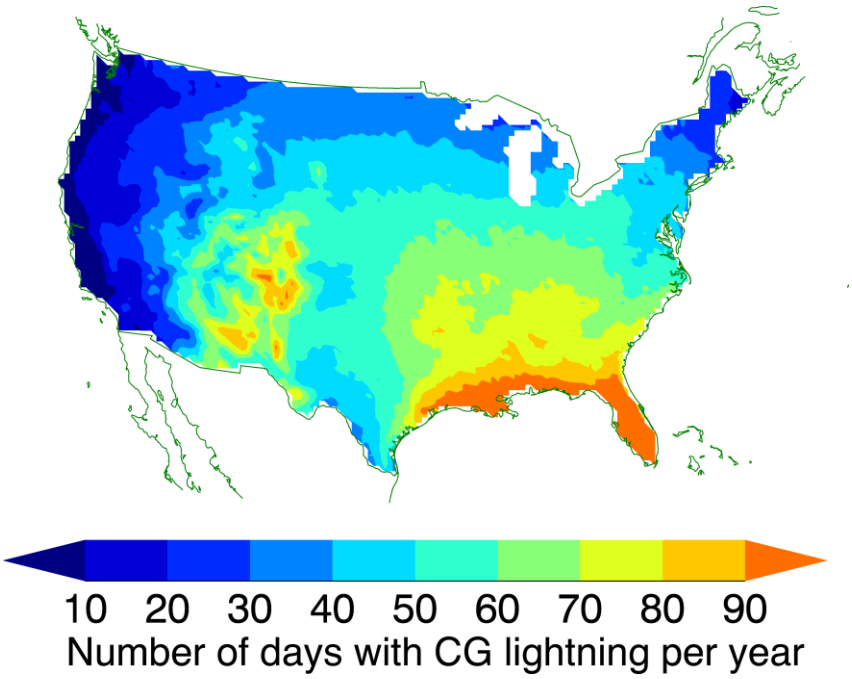

Figure 3. Number of days with NLDN detected cloud-to-ground (CG) lightning per model grid cell per year during 2005-2014. The lightning occurrences are calculated using the REAM grid resolution.

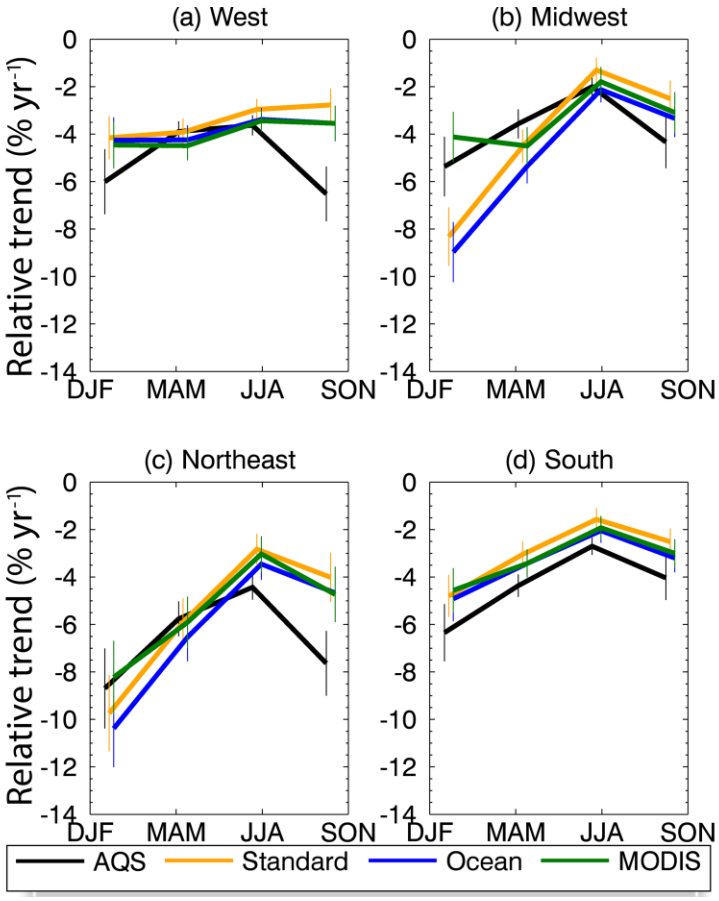

Figure 4. Seasonal relative trends of NO_2 calculated from the AQS in situ measurements ("AQS", black line) and those derived from different OMI VCD data ("Standard", orange line; "Ocean", blue line; "MODIS", green line). The error bars represent ~~95%~~95th percentile confidence intervals.

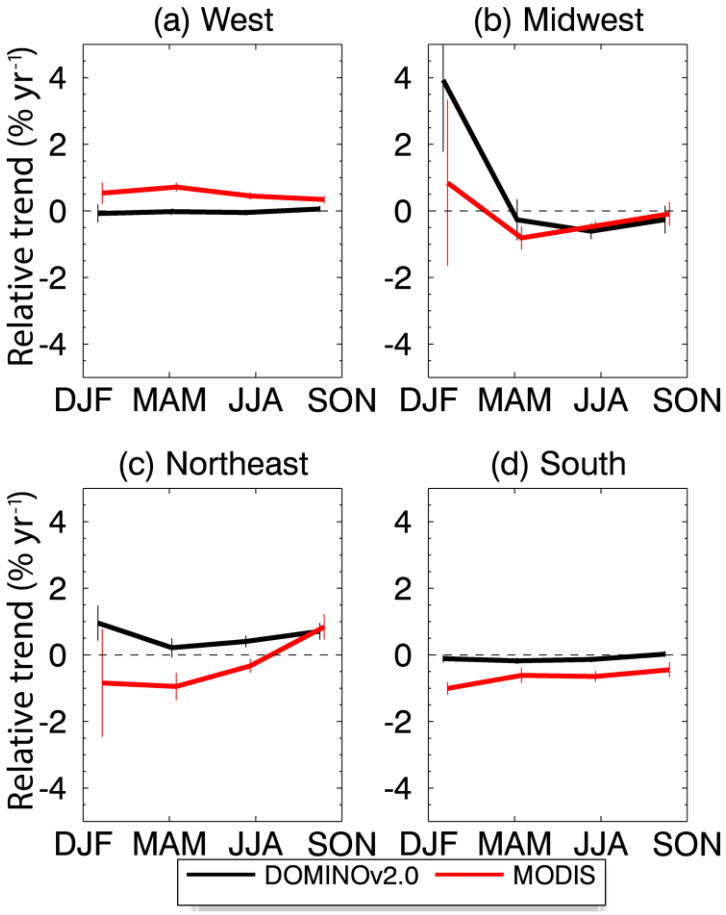

Figure 5. Seasonal relative albedo trends of OMI (black line) and MODIS (red line) surface reflectance products, coincident with AQS in situ data used in Figure 5. The error bars represent ~~95%~~95th percentile confidence intervals.

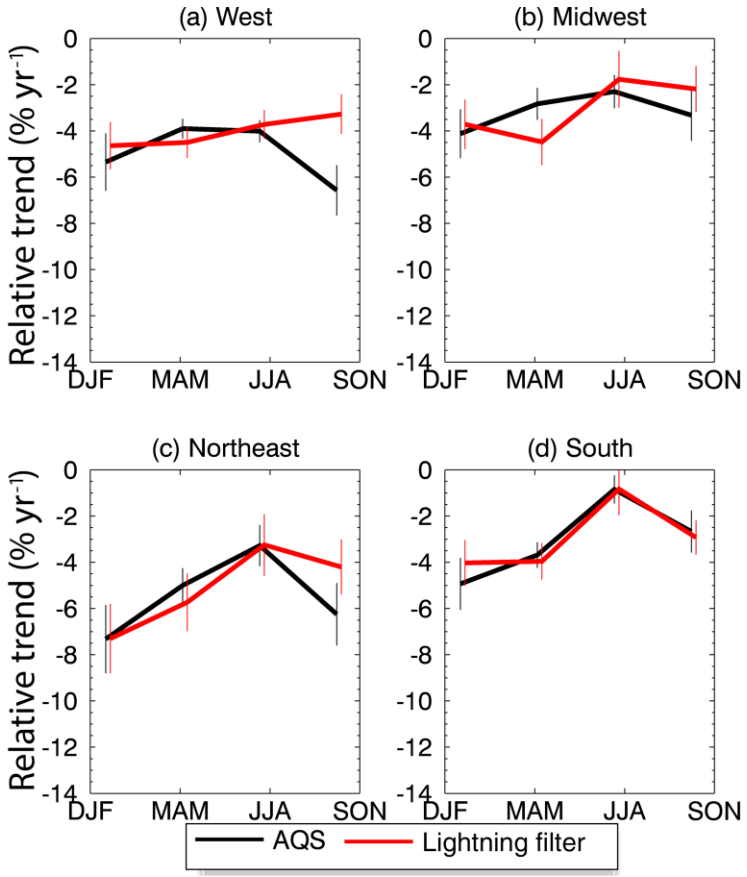
(a) West
(b) Midwest
(c) Northeast
(d) South
Relative trend (% yr-1)
0
-2
-4
-6
-8
-10
-12
-14
DJF
MAM
JJA
SON
AQS
Lightning filter

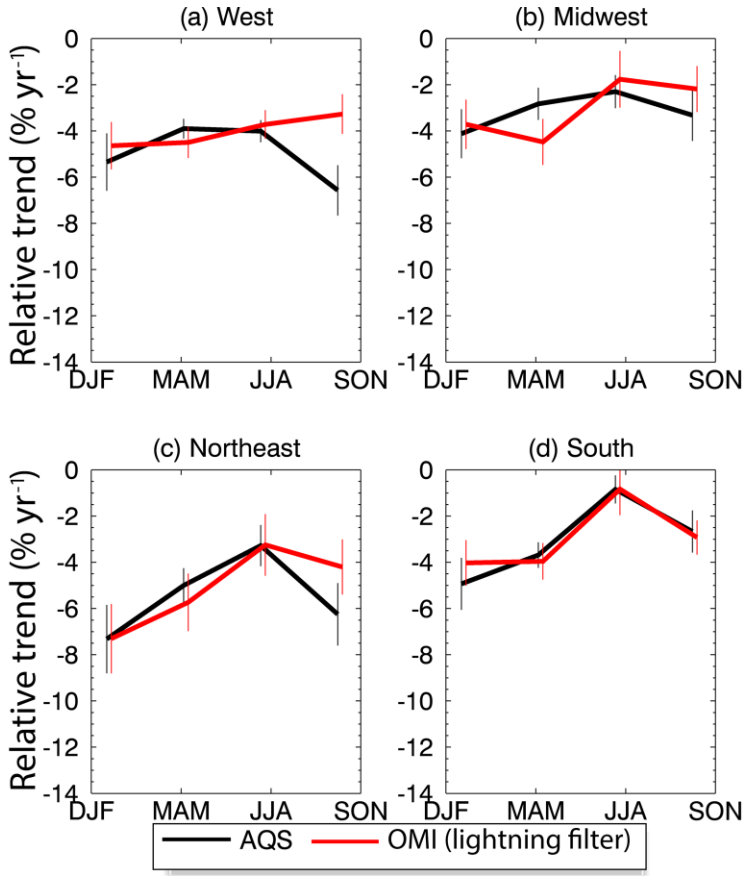

Figure 6. ~~Same as Figure 5 but for coincident~~ Seasonal relative trends of NO_2 calculated from the AQS ~~(~~in situ measurements ("AQS", black line) and those derived from OMI data ~~(red line)~~ after applying the lightning filter~~.~~ ("OMI (lightning filter)", red line). The error bars represent 95th percentile confidence intervals. The coincident data points are less than those used in Figure 5 and therefore the AQS trends are not the same.

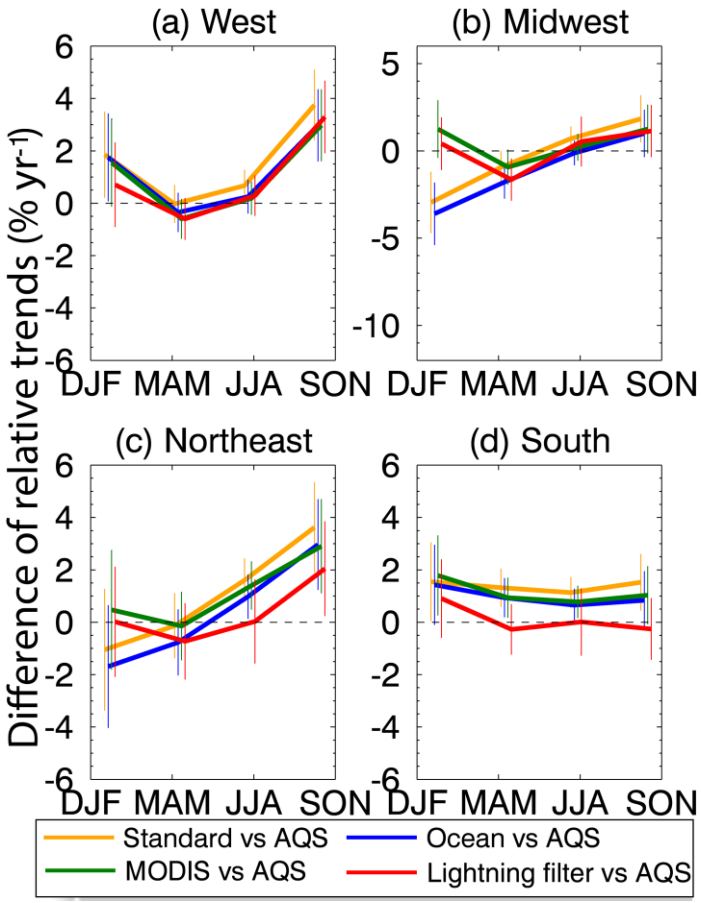

Figure 7. Seasonal differences of OMI-based relative trends from those computed from AQS in situ data. The error bars represent 95th percentile confidence intervals. The relative trends are shown in Figs. ~~6~~4 and ~~8~~6. The figure legends are the same as in Figs. ~~6~~4 and ~~8~~6 but with the AQS trends subtracted from the OMI-based trends.

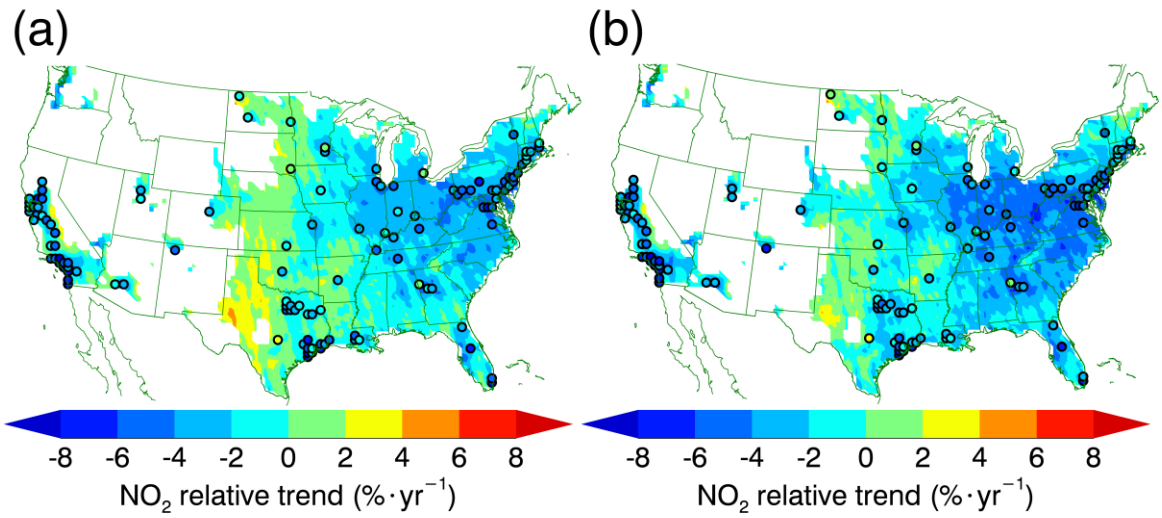

Figure 8: Annual relative trends of OMI-based NO_2 for "Standard" (a) and for "Lightning filter" (b) as the colored background. Black bordered circles indicate corresponding AQS NO_2 trends. Grid cells with 2005-2014 mean NO_2 VCDs < $1x10^{15}$ molecules cm^{-2} are excluded in the analysis and are shown in white.

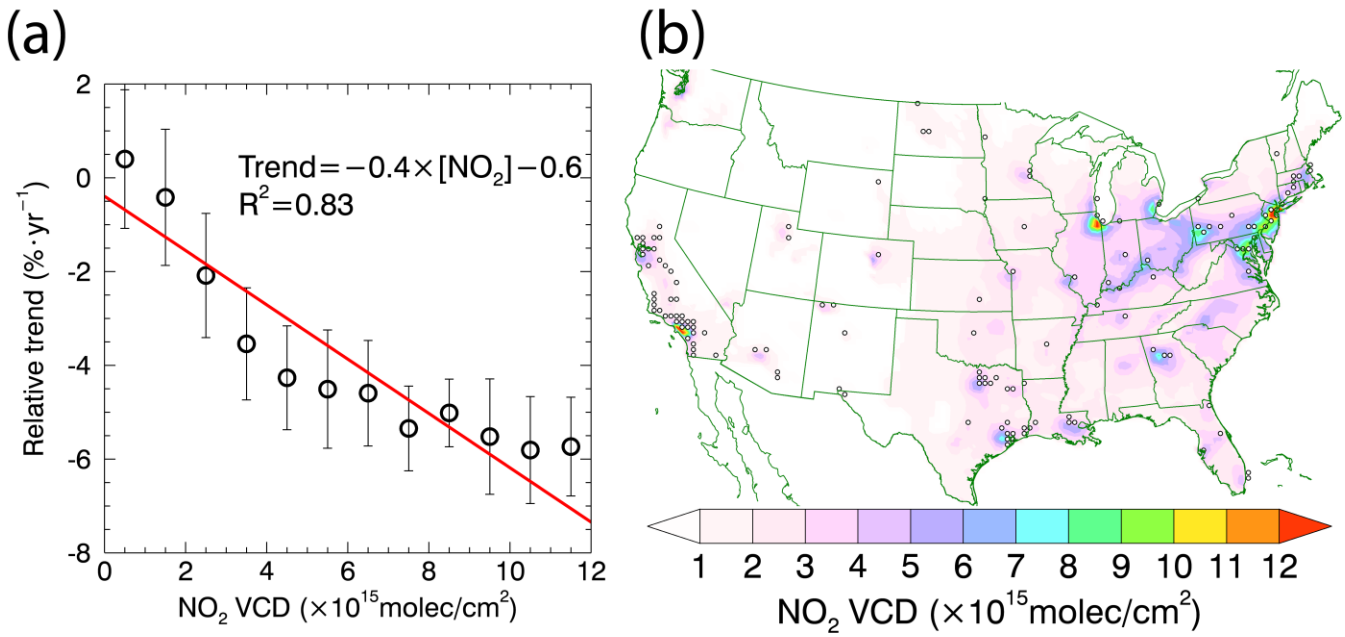

Figure 9. (a) The "Lightning filter" OMI-based NO_2 relative trend as a function 2005-2014 averaged OMI tropospheric NO_2 VCD binned every $1 \times 10^{15} molec/cm^2$. ~~Red~~The error bars represent 95th percentile confidence intervals. The red line shows a least-squares regression. (b) The distribution of 2005-2014 averaged OMI tropospheric NO_2 VCD. Black bordered circles represent AQS sites. The corrected OMI tropospheric NO_2 data ("Lightning filter") are used.

Table 1. Annual relative trends calculated with coincident data and all available data. ~~95%~~The 95th percentile confidence intervals from Mann-Kendall method are also listed.

Region	Annual relative trends of coincident data (% yr^{-1})				Annual relative trends using all data (% yr^{-1})			
	Standard		Lightning filter[a]		Standard		Lightning filter	
	AQS	OMI	AQS	OMI	AQS	OMI[b]	AQS	OMI[b]
West	-4.1±0.5	-3.2±0.4	-4.2±0.5	-3.8±0.4	-4.1±0.5	-0.9±0.4	-4.2±0.5	-2.0±0.3
Midwest	-3.4±0.5	-3.6±0.4	-2.8±0.6	-3.1±0.5	-2.5±0.5	-0.9±0.4	-2.2±0.5	-1.8±0.4
Northeast	-5.8±0.5	-5.0±0.5	-5.2±0.6	-5.3±0.7	-4.7±0.5	-3.0±0.4	-4.1±0.5	-3.1±0.5
South	-3.8±0.4	-2.7±0.3	-3.0±0.5	-3.0±0.5	-3.5±0.4	-0.2±0.4	-3.0±0.5	-0.9±0.3
Nationwide	-4.3±0.4	-3.5±0.3	-4.1±0.4	-3.9±0.3	-4.0±0.4	-0.7±0.3	-3.9±0.4	-1.5±0.2

[a] These data include the three corrections of this study, namely, ocean trend correction, MODIS albedo update, and ~~lighting~~lightning filter screening.

[b] The spatial coverage is shown in Figure 1.